AN ABSTRACT OF THE THESIS OF

Andrew W. Otto for the degree of Master of Science in Mechanical Engineering
presented on April 19, 2017

Title: Experimental Characterization of Saw Chain Cutting Performance

Abstract approved:

_____

John P. Parmigiani

Chainsaw users value cutting performance and safety. Knowledge of the forces exerted during sawing are necessary to understand and improve the cutting performance of saw chain. Additionally, cutting forces can be used to form metrics for evaluating performance tradeoffs when using a safety (*i.e.* low-kickback) saw chain *versus* a standard chain. The presented work investigates material and operational parameters influencing cutting forces through construction of a custom test stand and analysis using multiple linear regression. The experimental techniques are then applied in a comparison study of several commercially available low-kickback and non-low-kickback saw chains. Test methods were formed that successfully account for variations in workpiece physical properties (moisture content and density) as well as an observed cutting overload phenomenon. Maximum cutting efficiency was found to be governed by an operational parameter defined as the overload depth-of cut. Additionally, important interactions were observed between depth-of-cut with both workpiece moisture content and density. Three different low-kickback saw chains were compared to a non-low-kickback saw chain in both nose-clear down bucking and boring cutting modes. In down bucking, the best performing low-kickback saw chain had negligible differences in cutting forces compared to the non-low-kickback saw chain. In the boring cutting mode, professional saw chain had distinctly reduced operator effort (*i.e.* feed force) and greater cutting efficiency than the low-kickback chains. The presented testing and analysis methods

provide an experimental toolkit that can be used for evaluating the cutting performance of current saw chain offerings or to aid the development of new chain designs.

Experimental Characterization of Saw Chain Cutting Performance

by
Andrew W. Otto

A THESIS

submitted to

Oregon State University

in partial fulfillment of
the requirements for the
degree of

Master of Science

Presented April 19, 2017
Commencement June 2017

Master of Science thesis of Andrew W. Otto presented on April 19, 2017

APPROVED:

_____

Major Professor, representing Mechanical Engineering

_____

Head of the School of Mechanical, Industrial and Manufacturing Engineering

_____

Dean of the Graduate School

I understand my thesis will become part of the permanent collection of Oregon State University libraries. My signature below authorizes release of my thesis to any reader upon request.

_____

Andrew W. Otto, Author

ACKNOWLEDGEMENTS

The author would like to thank his advisor John Parmigiani for providing the opportunity to explore the area of experiment design and product testing. Additionally, the support from Mike Harfst, Matthew Cunnington, and Andy Phan at Blount International for general and technical guidance in all matters related to saw chain was greatly appreciated. Finally, my time at Oregon State would not have been possible without the generous support of my wonderful sponsors—my parents Ed and Anna.

CONTRIBUTION OF AUTHORS

Andrew W. Otto was the lead graduate student and was responsible for machine design and construction, testing, analysis, figure creation, and text preparation for both manuscripts. Levi J. Suryan performed testing for the second manuscript. John P. Parmigiani was the principal investigator, research advisor, and prepared text for both manuscripts.

TABLE OF CONTENTS

Page

1 Introduction....1

2 Velocity, Depth-of-cut, and Physical Property Effects on Saw Chain Cutting....3

2.1 Abstract.... 4

2.2 Nomenclature.... 4

2.3 Introduction.... 5

2.4 Experimental.... 8

2.5 Results and Discussion.... 16

2.6 Conclusions.... 28

3 Cutting Performance Comparison of Low-Kickback Saw Chain....30

3.1 Abstract.... 31

3.2 Introduction.... 31

3.3 Materials and Methods.... 33

3.4 Results.... 42

3.5 Discussion.... 48

3.6 Conclusions.... 49

4 Conclusion....51

5 Bibliography....53

LIST OF FIGURES

Figure		Page
Figure 2.1	A schematic of a chainsaw cutting a workpiece showing the measured cutting parameters of drive torque and velocity, feed force and velocity, and cutting force	8
Figure 2.2	Saw chain terminology	9
Figure 2.3	Mechanical components of the saw chain test apparatus	10
Figure 2.4	Test apparatus power head	11
Figure 2.5	Test apparatus work holding system	12
Figure 2.6	Grain orientation of the four timbers (A–D) used in testing	13
Figure 2.7	An example of force magnitudes as functions of time for a single cut in (a) a workpiece without knots or other defects and (b) a workpiece with a knot	15
Figure 2.8	Histograms, corresponding to the data of Figure 2.7, of cutting-force magnitudes showing the number of samples (i.e. data points measured during a single cut) in each of 15 equally-spaced intervals for (a) a workpiece without knots or defects and (b) a workpiece containing a knot. The labeled force magnitude is defined as the characteristic force value for the cut	15
Figure 2.9	Measured chain force, cutting force, and feed force versus depth-of-cut showing two linear regions	18
Figure 2.10	Interaction of (a) moisture content and (b) density with depth-of-cut on affecting chain force magnitude for the three force cases	24
Figure 2.11	Cutting forces and cutting efficiency versus depth-of-cut with the overload point and depth gauge setting indicated	27
Figure 3.1	Saw chain terminology and low-kickback saw chain elements (a) professional, non-low-kickback chain, (b) bumper tie strap low-kickback chain, (c) dumper drive link low-kickback chain	34

LIST OF FIGURES (Continued)

Figure		Page
Figure 3.2	Increase in depth-of-cut as cutter links traverse the guide bar nose	35
Figure 3.3	A diagram of a chainsaw performing a boring cut showing the measured cutting parameters of drive torque and velocity, chain tension, feed force and velocity, and cutting force	36
Figure 3.4	Testing machine used to measure cutting forces and control cutting rates during experiments	38
Figure 3.5	End-grain orientations for down bucking and boring cutting modes	38
Figure 3.6	(a) Representative cutting force waveform collected during a single cut, (b) the histogram method used to extract the effective cutting force (192.5 N in this case) from the force waveforms	40
Figure 3.7	Root mean square error (RMSE) of feed force (F_F) as a function of overload depth of cut (δ_{OL}) for each chain used in the low-kickback study in down bucking. Minimums are indicated using solid dots on each line	45
Figure 3.8	Chain force (F_{CH}), cutting force (F_C), feed force (F_F), and cutting efficiency (η) plotted versus depth of cut (δ) for each of the four chains (A, B, C, D) used in the low-kickback comparison study for both the down bucking (left column, a–d) and boring (right column, e–h) cutting modes	47

LIST OF TABLES

Table		Page
Table 2.1	Calculated cutting parameters	10
Table 2.2	Measured moisture content and density	17
Table 2.3	Regression coefficients, parameters, and fit to data	20
Table 2.4	Effect of changing predictor variable magnitude	22
Table 3.1	Calculated cutting parameters	37
Table 3.2	Measured workpiece moisture content and density	43
Table 3.3	Regression model coefficients and fit, down bucking	44
Table 3.4	Regression model coefficients and fit, boring	44
Table 3.5	Selected overload depth-of-cut values, down bucking	46

1 INTRODUCTION

Chainsaws are a common power tool used for many wood-cutting tasks ranging from personal property upkeep to commercially harvesting timber in the forest. Regardless of the task, all chainsaw users value cutting performance with respect to chainsaw size—as high power-to-weight ratio saws ultimately increase saw portability and reduce operator fatigue. Manufacturers are particularly interested in improving the cutting performance of saw chain to reduce power requirements, and therefore size, of the chainsaw power head. To guide improvements in cutting performance, engineers require an understanding of saw chain cutting mechanics. Cutting mechanics, the process of force generation and material removal by a cutting tool, is governed by workpiece properties, tool geometry, and operating conditions (*e.g.* chain speed and depth-of-cut).

Understanding saw chain cutting mechanics poses several challenges. Existing work in wood cutting mechanics, while well established, lacks many aspects that are important to wood cutting with a chainsaw. Traditional wood cutting investigations focus on orthogonal cutting using a simple wedge-shaped tool, where the tool spans the entire width of the workpiece and the cutting edge is held perpendicular to the cutting direction. While this simplified scenario elicits many of the key factors governing cutting mechanics, it does not capture several of the complexities present in chain sawing. Chain sawing differs from the orthogonal cutting situation because material is removed from three surfaces forming a kerf, the cutting edge is not perpendicular to the cutting direction, cutter geometries are more complex than simple wedges, and the links of the chain are free to rotate in the plane of the chainsaw guide bar while cutting.

Interest in saw chain cutting mechanics has varied since the chainsaw saw widespread adoption for timber harvesting in the late 1940s [1]. Overall, the existing chainsaw cutting literature is dated, experiment-based, and does not generalize well for comparisons of different chains. Early work by McKenzie [2] identified the influence of cutter geometry (rake angle, top plate bevel angle, and depth gauge clearance) as well as depth-of-cut on cutting forces with different saw chains. Other works have examined the influence of cutter geometry on cutting forces, but these

focused on single saw chain teeth rather than the entire cutting chain [3,4]. With respect to full chain testing, Pahlitszch and Peters [5,6] were the first to consider the effects of cutter geometry, feed rate, and workpiece properties (moisture content, specifically) on cutting forces in a single study. The work of Reynolds *et al.* [7,8] formed a linear model from experimental data using operating parameters such as depth-of-cut and chain velocity to predict cutting power requirements for different chains. Stacke [9] combined measurements taken from single tooth experiments with a dynamic model of the chain to investigate the influence of chain parameters such as chain speed, depth-of-cut, rivet friction, chain mass, and cutter shape on cutting forces. Lacking from the prior works in saw chain cutting are considerations for variability in workpiece properties. Instead, researchers have focused on tightly controlling wood conditions to limit the influence of wood heterogeneity on experimental results. Fortunately, recent work in orthogonal cutting demonstrates that tracking wood mechanical properties (*e.g.* modulus, strength, and toughness) as well as physical properties (*e.g.* density and moisture content) can accurately predict changes in cutting forces [10].

The goal of the work presented herein is to expand the established testing methods for saw chain by including a measure of workpiece variability and to provide a generalized method for analyzing factors influencing cutting performance by using multiple linear regression. Attention is given to characterizing workpiece variability using quick and convenient measures, a requirement typical of industry product-testing environments. This thesis is a collection of two works: (1) a description of a custom saw chain testing machine built to perform cutting experiments and subsequent experimentation to characterize saw chain cutting performance using multiple linear regression and (2) utilization of the testing techniques to perform a comparison study between a set of commercially available low-kickback and non-low-kickback saw chains.

2 VELOCITY, DEPTH-OF-CUT, AND PHYSICAL PROPERTY EFFECTS ON SAW CHAIN CUTTING

Andrew W. Otto, John. P. Parmigiani

BioResources
North Carolina State University
Dept. of Forest Biomaterials
College of Natural Resources
Campus Box 8005
Raleigh, North Carolina 27695-8005
Volume 10, Issue 4

2.1 Abstract

A better understanding of saw-chain cutting mechanics is needed for more efficient chainsaw designs. The effects of varying key parameters such as workpiece moisture content, workpiece density, cutting velocity, and depth-of-cut, while established for other types of cutting, are largely unexplored and/or unpublished for saw chains. This study contributes to filling this gap through experimentation and analysis. Experiments were conducted using a custom-built saw-chain testing apparatus to measure relevant forces over a range of workpiece moisture contents, workpiece densities, cutting velocities, and depths-of-cut. Analysis consisted of fitting linear regression models to experimental data, identifying trends, and exploring optimum cutting conditions. Results showed that over the range of values included in the study, workpiece moisture content and density had effects that depended on the depth-of-cut. Cutting velocity had a small effect, and depth-of-cut had a large effect. All trends fit well with linear models; however, depth-of-cut required one linear fit for small-to-mid values and a second fit for mid-to-large values. Maximum efficiency was found to occur at a depth-of-cut equal to the transitional value between fits. These results provide basic relationships that can lead to the more effective and efficient use and design of chainsaws.

2.2 Nomenclature

F	Force magnitude (N)
F_C	Cutting force (N)
F_{CH}	Chain force (N)
F_F	Feed Force (N)
F_T	Chain tension (N)
k	Shear yield strength (N/m^2)
L	Length of cut (mm)
MC	Workpiece moisture content (%)
n	Number of drive sprocket teeth
P	Saw chain pitch (mm)
Q	A function of friction coefficients and tool geometry (dimensionless)
R	Specific work of surface separation (J/m^2)
S	Saw chain tooth spacing
T_M	Drive-sprocket torque (Nm)
V_C	Cutting velocity (m/s)

V_F	Feed velocity (m/s)
w	Kerf width (m)
β_i	Regression model coefficients (varies)
δ	Depth of cut (mm)
δ_{DG}	Saw chain depth gauge setting (mm)
δ_{OL}	Overload depth-of-cut (mm)
ΔF	Change in force magnitude (N)
ΔPV	Change in the varying predictor variable (varies)
γ	Shear yield strain (dimensionless)
η	Cutting efficiency (mm^2/J)
ρ	Workpiece density (kg/m^3)
ω	Drive-sprocket angular velocity (radians/s)

Throughout the text, a symbol with an over-bar (*e.g.* $\bar{x}$) denotes a mean value, and a symbol with an asterisk superscript (*e.g.*, x^*) denotes a value less its mean value (*i.e.*, $x^* = x - \bar{x}$).

2.3 Introduction

Whether harvesting forest trees, performing storm cleanup, clearing trees, or mitigating wildfires, a chainsaw is a common tool for cutting wood. Increased efficiency and effectiveness are highly desired by both professional and home users. In particular, chainsaw manufacturers are interested in increasing energy efficiency for cordless electric chain saws in order to maximize operating performance and duration due to the relatively low power density of batteries. Designing chainsaws to meet these needs requires an understanding of chainsaw cutting mechanics, which typically involves experimentation. This is complicated by variations in the physical properties (*e.g.*, density) of the wood workpieces used in testing. Two important aspects of saw chain cutting mechanics are the roles of chain velocity and depth-of-cut. Changes in chain velocity and depth-of-cut can affect cutting forces and thus affect energy consumption and efficiency. Significant published research exists regarding the effects of wood specimen variability, cutting velocity, and depth-of-cut, but most studies have involved orthogonal cutting and rigid-cutter sawing (*i.e.*, sawing in which individual cutter teeth do not move relative to each other, as in band saw blades and circular saw blades but not saw chains). Thus, a significant gap in understanding exists regarding these effects in saw chain cutting.

Workpiece physical properties play a large role in woodcutting. As a natural material, wood exhibits a high degree of variation that complicates the effect of material properties on cutting. Studies in orthogonal cutting and rigid-cutter sawing have shown that cutting forces increase with density and decrease with moisture content up to the fiber saturation point [11–13]. However, moisture content and density alone are inadequate predictors of cutting force. The orthogonal cutting and rigid-cutter sawing of different species with the same moisture content and density will generally result in different cutting forces [12–14]. More recent research has made use of other physical properties to describe the influence of the work piece on cutting forces. Naylor *et al.* [10] successfully formed a species-independent linear regression model of cutting forces for rigid-cutter sawing using material strength and fracture toughness. However, the authors know of no published work specifically for saw chain that quantifies the effect of physical properties on cutting forces.

A significant body of research exists regarding the effect of cutter velocity in woodcutting. In orthogonal cutting, it is widely accepted that cutting velocity has little to no impact on cutting forces [11,12,15]. However, in the area of rigid-cutter sawing, Koch [13] suggests several effects that can cause cutting forces to become velocity-dependent—acceleration of chips out of the saw kerf, strain rate-dependent failure of wood, and changes in frictional behavior between the tool and work piece at varying velocities. Also in the area of rigid-cutter sawing, Orlowski *et al.* [16] found that chip acceleration must be accounted for in the characteristically higher speeds of band sawing and circular sawing to accurately predict power requirements, suggesting that cutting velocity influences cutting forces at high speeds. Regarding saw chains, Stacke [9] developed a fully dynamic model for the motion paths of saw chain cutters within the kerf and illustrated the influence of chain velocity and inertia on the saw chain cutting process. His findings suggest that chain momentum acts to smooth the motion path of a cutter, reducing cutting forces and energy consumption. Additionally, Stacke showed that higher chain velocities increase the drive torque on a free running chain due to chain-bar friction, reducing cutting efficiency. Heinzelmann *et al.* [17] also states that frictional losses in the chainsaw cutting system increase with chain velocity, and therefore claims that achieving reasonable battery life for battery-powered applications requires the chain to run at lower speeds than those typical of gasoline-powered saws. However,

this research does not conclusively establish that reduced cutting velocity will improve overall cutting efficiency. For example, research has not been conducted to determine whether the reduced frictional losses occurring at low cutting velocities will translate into overall gains in chainsaw efficiency or if they will be offset by the rough-cutting inefficiency of a slow-moving, low-momentum saw chain. The authors found no published literature defining an optimum cutting velocity for saw chain.

Research on the effect of depth-of-cut exists for orthogonal cutting, rigid-cutter sawing, and, to a lesser extent, for saw chain cutting. For both orthogonal cutting and rigid-cutter sawing under typical operating conditions, a linear relationship between cutting force and depth-of-cut has been shown to work well by a number of researchers [11–13,15,18–22]. Under non-typical rigid-cutter sawing conditions, when excessive depths of cut are used, cutting forces and energy consumption have been found to increase in a non-linear fashion [13]. This non-linear behavior is loosely correlated with the effects of chip transport and cutter geometry, but lacks experimental data for confirmation. Also in the area of rigid-cutter sawing, Oehrli [23] reported an optimal value of depth-of-cut with respect to energy consumption for a circular saw. Little research has been conducted on the effect of depth-of-cut for saw chain. It has been found that when depth-of-cut roughly equals the depth gauge, sliding friction between the saw chain and wood increases greatly [2]. Regression models based on experimental data have shown that cutting forces increase with increasing depth-of-cut [7]. Also, it has been determined that cutting rates increase dramatically when the depth gauge setting is enlarged [24]. However, no published literature has been found that defines the relationship between depth-of-cut and cutting efficiency for saw chain or for identifying an optimum depth-of-cut.

The work presented in this paper considers the effects workpiece moisture content, workpiece density, cutting velocity, and depth-of-cut on saw-chain cutting forces and saw-chain cutting efficiency. Moisture content and density were measured for each offcut. Cutting velocity and depth-of-cut were specified over a range appropriate for a battery-powered electric chain saw. Cutting forces were measured using a test apparatus constructed by the authors specifically for saw chain. Key aspects

of this paper include effectively modeling the effects of moisture content, workpiece density, cutting velocity, and depth-of-cut on cutting forces using a multiple linear regression model, using this model to demonstrate trends in cutting forces and cutting efficiency, and identifying conditions corresponding to optimum cutting efficiency.

2.4 Experimental

2.4.1 Terminology

The cutting parameters that were measured in this study are illustrated in Figure 2.1, a schematic of a chainsaw cutting a workpiece. The cutting force (F_C) and the feed force (F_F) are the components of the reaction force acting on the workpiece in directions parallel to the guide bar and normal to the guide bar, respectively. Torque (T_M) is the input torque applied to the drive sprocket to propel the saw chain, and ω is the angular velocity of the drive sprocket. The force (F_T) is the non-cutting chain tension (*i.e.*, chain not in contact with the workpiece). The feed velocity (V_F) is the velocity of the guide bar into the cut (*i.e.*, normal to the guide bar for the cuts performed in this work).

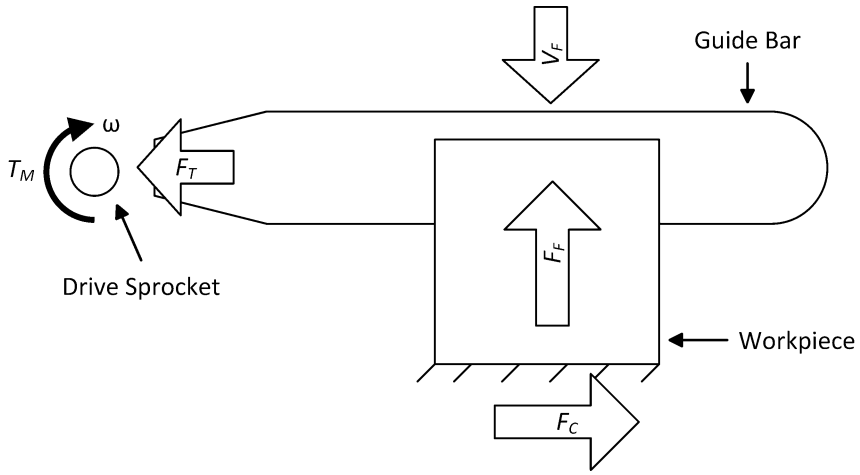

Figure 2.1 A schematic of a chainsaw cutting a workpiece showing the measured cutting parameters of drive torque and velocity, feed force and velocity, and cutting force

Saw chain terminology is illustrated in Figure 2.2 for a typical saw chain as used in this study. This saw chain consists of three types of links connected by rivets: drive

links, cutter links, and tie straps. Drive links engage the drive sprocket to propel the chain and also slide through a notch in the guide bar to constrain the saw chain to move about the guide bar periphery. Cutter links consist of a cutter tooth and a depth gauge. Cutter teeth curl above the cutter-link body and alternate in orientation between teeth pointing to the left and pointing to the right. The cutter teeth perform the actual cutting by removing a chip from the work piece. The depth gauge limits the thickness of the cut chip. Tie straps connect drive links and cutter links. The distance between the top of the depth gauge and the sharp edge of the cutter tooth is the depth gauge setting (δ_{DG}). Tooth spacing (S) is defined as the number of rivets between cutter teeth of the same orientation and is equal to eight for a standard sequence chain. Chain pitch (P) is defined as half the distance between the end of a cutter link and the corresponding end of an adjacent tie strap.

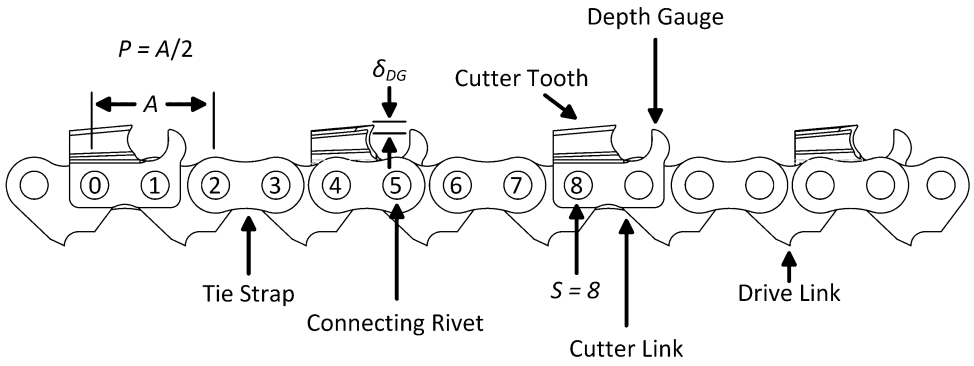

Figure 2.2 Saw chain terminology

The parameters defined above were used to calculate the three quantities listed in Table 2.1. The chain force (F_{CH}), given by Eq. 2.1, is the cutting chain tension (i.e., the force applied to the chain by the drive sprocket during cutting). It can be calculated from the drive sprocket torque, the chain pitch, and the number of sprocket teeth (n). The cutting velocity (V_C), given by Eq. 2.2, is the velocity of the moving saw chain and can be calculated from the sprocket angular velocity, the chain pitch, and the number of teeth on the sprocket. The depth-of-cut (δ), given by Eq. 2.3, is the average thickness of a chip removed by an individual cutter tooth and can be calculated from the chain velocity, feed velocity, chain pitch, and tooth spacing. Note the depth gauge of the saw chain only acts to inhibit depth-of-cut greater that the depth gauge setting and does not independently determine depth-of-cut.

Table 2.1 Calculated cutting parameters

Parameter	Calculation	
Chain Force (N)	$F_{CH} = \frac{\pi\, T_M}{1000\, Pn}$	(2.1)
Chain Velocity (m/s)	$V_C = \frac{1000\, Pn\omega}{\pi}$	(2.2)
Depth-of-cut (mm)	$\delta = \frac{V_F}{V_C} P\, S$	(2.3)

2.4.2 Test Apparatus

A test apparatus was designed and built for this study. The apparatus consists of four components: a power head, a motion system, a work holding system, and a data acquisition system. The three mechanical components are shown in Figure 2.3.

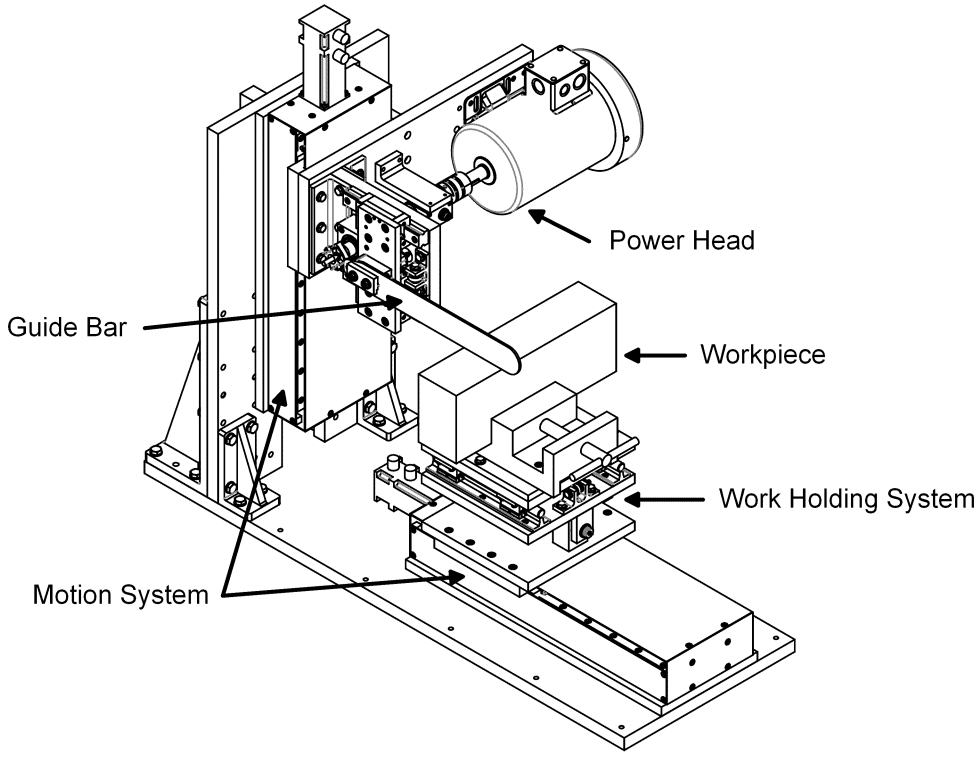

Figure 2.3 Mechanical components of the saw chain test apparatus

The power head, illustrated in Figure 2.4, propels the saw chain and measures several test parameters. A 1.5 kW AC motor was used, corresponding to the power

typically available for smaller gasoline-powered and electric battery-powered saws. The motor is capable of speeds up to 7,000 RPM and is controlled through a variable frequency drive.

The guide bar is mounted to linear bearings whose motion is opposed by a load cell (670 N measuring range) that measures chain tension. Standard commercial guide bars and chains can be used. Lubricating oil for the saw chain is provided in the same manner as a typical commercial chainsaw, through the orifice on the guide bar. Chain tension is adjusted with the screw system common to typical commercial chainsaws. An inline torque transducer (20 Nm measuring range) with optical encoder, located between the motor and the drive sprocket, measures input torque and drive sprocket angular velocity.

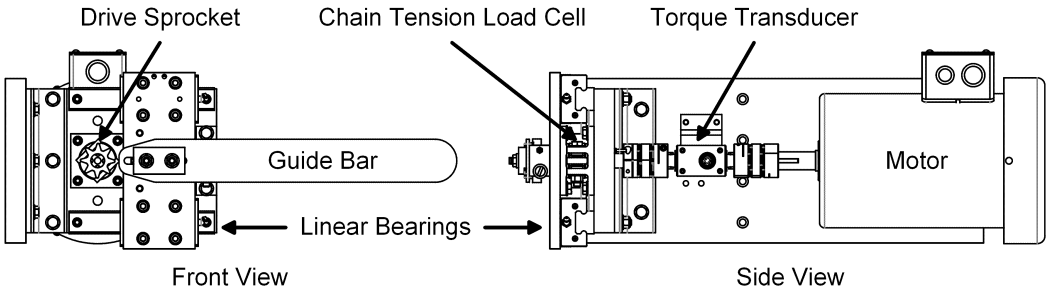

Figure 2.4 Test apparatus power head

The work holding system, shown in Figure 2.5, holds the workpiece and measures the cutting force and feed force. A drill-press vise is used to hold the workpiece. The cutting force is measured using a linear bearing system opposed by an S-beam load cell (1300 N measuring range), similar to that of the chain-tension measurement system on the power head. The feed force is measured using a pivot mechanism and S-beam load cell (450 N measuring range).

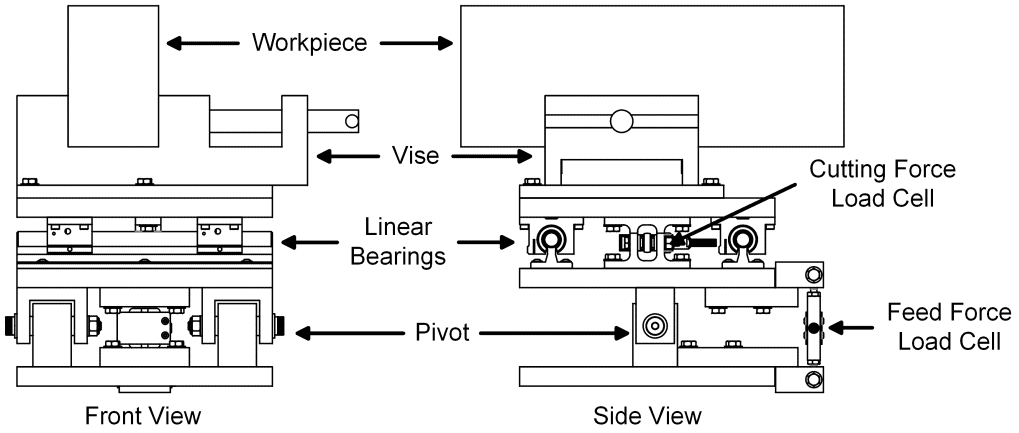

Figure 2.5 Test apparatus work holding system

The motion system is comprised of two identical linear motion slide tables. These tables move vertically and horizontally relative to, and in the plane of, the bar and have a maximum linear speed of 83 mm/s. They are driven by a 400 W servo motor. The vertical slide table provides the mounting surface for the power head. An incremental optical encoder is used for feedback control and measurement of feed velocity. The horizontal axis provides the mounting surface for the work holding system.

The data acquisition system records all measurements and saves the output to disk after each cut. Machine control and data acquisition are accomplished using a National Instruments (USA) CompactRIO programmable automation controller. Force channels are sampled at 2 kHz and filtered using a 200 point moving average filter. A personal computer with LabVIEW (National Instruments) provides the user interface to the machine.

2.4.3 Materials

Workpieces for all testing were obtained from Douglas-fir dimensional timbers. Each timber had a rectangular cross-section (90 by 140 mm), a length of 3.0 m, and was purchased from a local supplier. Four timbers were used, denoted A through D in Figure 2.6, and each was cut into four 0.75 m workpieces, sized to fit inside the safety enclosure of the test apparatus.

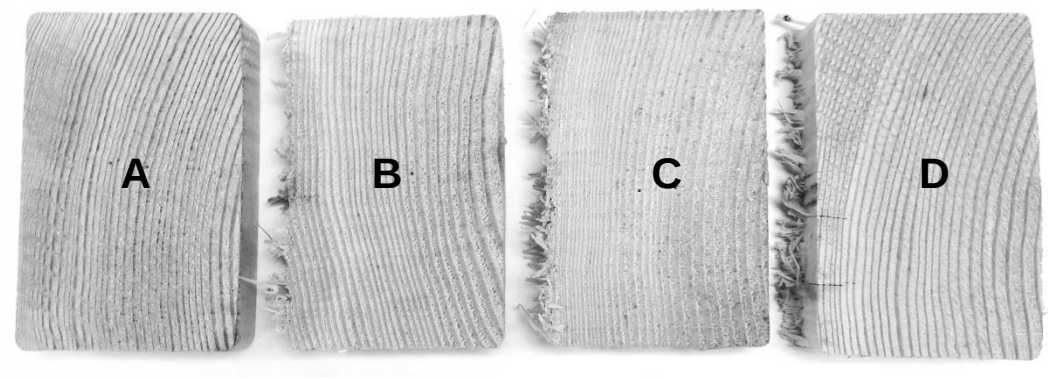

Figure 2.6 Grain orientation of the four timbers (A–D) used in testing

Each timber had roughly similar grain orientations with growth rings oriented vertically so that cuts were made perpendicular to the rings, thus passing through equal amounts of early and late wood. During testing, cuts on each 0.75 m workpiece were separated by 25 mm, giving a total of 20 offcuts per workpiece. Immediately following cutting, each offcut was labeled with an identification number for the purpose of visual inspection and to track the occurrence of knots.

2.4.4 Test Procedure

Each use of the test apparatus to complete a cut and collect data followed the same procedure. First, the guide bar and saw chain were installed on the power head. Next, the workpiece was oriented as shown in Figure 2.6 and secured in the vice of the work holding system such that the cut would occur at the desired location. Then the drive sprocket rotational velocity and feed velocity, as determined from the desired depth-of-cut and chain velocity using Eqs. 2.2 and 2.3, were set. Chain lubricating oil was applied at the desired rate. The non-cutting chain tension was then determined by calculating the average over a 2 second time period of the measured chain tension while the chain was free running (*i.e.*, driven by the drive sprocket rotating at the specified rotational velocity and without making contact with the workpiece). Adjustments to the chain tension, if necessary, were made using the screw adjustment on the power head. The weight of workpiece was measured. The desired feed velocity was then set and the cut was performed. Following cutting, the machine returned to its initial position and data were saved for post processing. Moisture content was measured immediately following each cut using a

Delmhorst J-2000 moisture meter by manually inserting the meter's probe into the center of the workpiece cut cross-section. The workpiece density corresponding to a cut was calculated by dividing the mass of the offcut by its volume. Mass was measured using a gram scale. Volume was measured using digital calipers.

2.4.5 Data Processing

Prior to analysis, several data processing steps were performed. Noise was removed from the cutting force data with a 200 point (0.1 second) moving-average filter. The effect of workpiece weight was removed from the feed force by subtracting the weight of the workpiece from the feed force measured during cutting. The increase in measured forces due to knots or other defects in the workpiece was addressed by using the modal value of force rather than the mean value. More specifically, during a cut in defect-free wood, forces remain approximately constant during cutting, and a simple mean value can characterize cutting forces accurately. However, when a knot or highly distorted grain is encountered in the work piece, force magnitudes increase, often significantly. This effect is illustrated in Figure 2.7 with representative data for the chain force, cutting force, and feed force.

Because the intent was to study the cutting of wood without including the presence of knots and other defects as an additional variable, this effect needed to be addressed. A simple mean value is not appropriate because it inherently results in force magnitudes above the defect-free values. The alternative method used was to calculate the most frequently occurring force magnitudes (the modal value). This approach is illustrated in Figure 2.8 and consisted of defining 15 equally spaced intervals spanning the minimum to maximum instantaneous force values occurring during the cutting period. The midpoint of the interval containing the greatest number of data points is defined as the characteristic force value for that cut. All force values were calculated using this method and all cuts, whether encountering knots or not, were included in the subsequent data analysis.

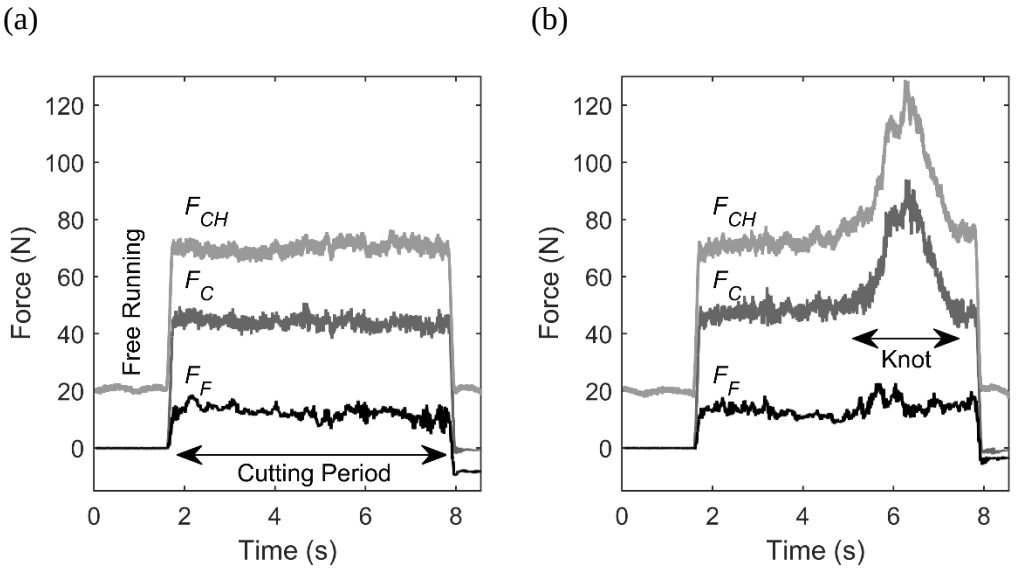

Figure 2.7 An example of force magnitudes as functions of time for a single cut in (a) a workpiece without knots or other defects and (b) a workpiece with a knot

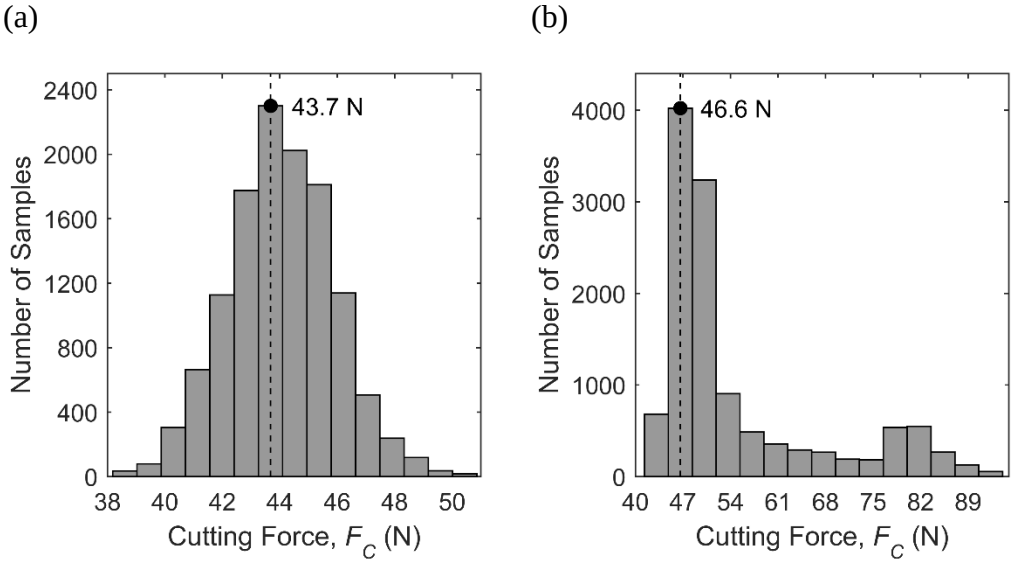

Figure 2.8 Histograms, corresponding to the data of Figure 2.7, of cutting-force magnitudes showing the number of samples (*i.e.* data points measured during a single cut) in each of 15 equally-spaced intervals for (a) a workpiece without knots or defects and (b) a workpiece containing a knot. The labeled force magnitude is defined as the characteristic force value for the cut

2.4.6 Data Analysis

The primary data analysis method used was multiple linear regression. The selected response variables were chain force, cutting force, and feed force. Four predictor variables were used for each response variable: the controlled (specified) variables of chain velocity and depth-of-cut and the uncontrolled (measured) variables of workpiece moisture content and workpiece density. For each of the three response variables, all single-factor predictor-variable main effects and two-factor predictor-variable interaction effects were considered as being possibly significant. Three-factor and higher interaction effects were all assumed to be negligible and were not considered.

2.5 Results and Discussion

2.5.1 Collected Data and Regression Model

Testing consisted of repeated cuts at varying chain velocities and depths-of-cut. Specifically, four chain velocities (3.81, 5.72, 7.62, and 9.52 m/s) and seven depths-of-cut (0.05, 0.15, 0.25, 0.35, 0.45, 0.55, and 0.65 mm) were specified. Each combination of chain velocity and depth-of-cut was repeated eight times for a total of 224 cuts. Workpiece moisture content and density were measured for all offcuts. Two replicates were made within each of the four 3.0 m timbers (A, B, C, and D), and runs were dispersed randomly to reduce systematic error. For all cuts, chain tension was held constant at 89 N (±5 N). Chain lubricating oil was applied at 5 mL/min as recommended by the manufacturer. The chain used had a 9.525 mm (3/8 in) pitch, a standard sequence, and a depth gauge setting of 0.635 mm. A six-tooth spur sprocket was used. All chains, bars, and sprockets used for testing were in a new, out-of-box condition. The chain was replaced halfway through testing to limit the effect of dulling on cutting force data.

Prior to determining coefficients for the regression models, the collected data were analyzed. The mean and standard deviation of moisture content (*MC*) and density (ρ) are given in Table 2.2. Overall, moisture content varied from 12.0% to 24.8%, and density from 500 kg/m^3 to 695 kg/m^3. The larger standard deviation in wood

density in workpiece C is attributed to a higher occurrence of knots compared with the other three workpieces.

Table 2.2 Measured moisture content and density

Timber	***MC* (%)**		**ρ (kg/m^3)**	
	Mean	Standard Deviation	Mean	Standard Deviation
A	18.4	1.46	561	23.7
B	17.8	1.28	521	20.4
C	22.7	2.10	556	31.8
D	23.4	0.23	541	16.9
All	20.6	2.86	544	28.4

Chain force, cutting force, and feed force, for each of the 224 cuts performed, is shown *versus* depth-of-cut in Figure 2.9. This data shows that the relationship between chain force and depth-of-cut was best described by two linear regions, one extending from small depth-of-cut to a depth-of-cut of approximately 0.45 mm and a second extending from 0.45 mm to a large depth-of-cut. Increased variance in cutting forces at larger depths of cut, as seen in Figure 2.9, can be attributed to the increased influence of moisture content and density on the cutting forces at higher depth of cut as well as a reduced ability to maintain cutting velocity near the machine's power limit, thus resulting in reduced ability to maintain constant depth of cut during a single cut. An analysis of force *versus* moisture content, force *versus* density, and force *versus* cutting velocity did not show similar bilinear behavior (*i.e.*, a simple linear fit was sufficient for all parameters except depth-of-cut). Similar increases in the rate-of-change of force at high depths-of-cut have been observed for saw chain cutting by McKenzie [2] and can be inferred for rigid-cutter sawing from the work of Koch [13]. However, using a bilinear approach is a new method for modeling this phenomenon.

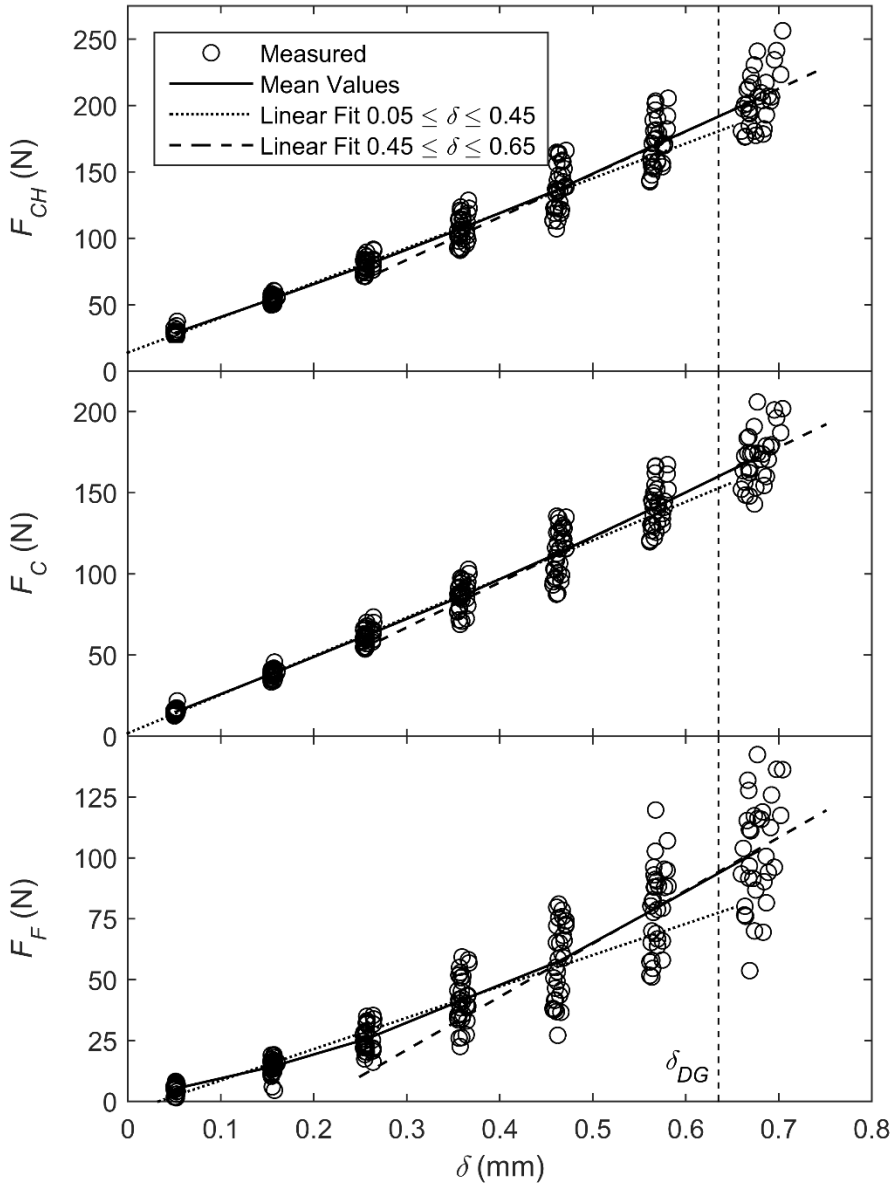

Figure 2.9 Measured chain force, cutting force, and feed force *versus* depth-of-cut showing two linear regions

With consideration for the bilinear behavior of the force *versus* depth-of-cut relationship, the regression equations for chain force, cutting force, and feed force were calculated. For each of the three forces, the same eight terms were included: a constant term, main effect terms for moisture content, density, and cutting velocity, two main effect terms for depth-of-cut (the second including the bilinear response), an interaction term for moisture content and depth-of-cut, and an interaction term

for density and depth-of-cut. Higher order terms and other interactions were not found to be significant based on their t-statistic with regressions containing those additional terms. Main effect terms and interaction terms were centered about mean values. Thus, the general form of the regression model is:

$$F_{CH},\ F_C, F_F = \beta_0 + \beta_1(MC^*) + \beta_2(\rho^*) + \beta_3({V_C}^*) + \beta_4(\delta^*) + \beta_5\langle\delta - \delta_{OL}\rangle + \beta_6(MC^*)(\delta^*) + \beta_7(\rho^*)(\delta^*)$$

where

$$\langle\delta - \delta_{OL}\rangle = \begin{cases} 0 & \text{if } \delta^* \le \delta_{OL} - \bar{\delta} \\ \delta - \delta_{OL} & \text{if } \delta^* > \delta_{OL} - \bar{\delta} \end{cases}$$

The β_i factors are the regression model coefficients, over-bars indicate mean values (*e.g.*, $\bar{\delta}$ is the mean value of depth-of-cut for all 224 cuts of the study), the asterisk superscripts refer to the indicated quantity minus its mean value (*e.g.*, $MC^* = MC - \overline{MC}$), and δ_{OL}, referred to as the overload depth-of-cut, is the depth-of-cut corresponding to the transition in the bilinear force response. Its value was calculated to provide the best fit for all three forces. The increase in force at high depths-of-cut is provided by the expression in Macaulay brackets $\langle\delta - \delta_{OL}\rangle$.

The regression model coefficients, mean values, overload depth-of-cut, and fit parameters are given in Table 2.3. The regression model provided excellent fits for each of the three forces. The R^2 values were all above 0.9, indicating that the regression models capture variance in the data very well. The F-statistic for each model was well above the critical value required for significance ($F_{7,216,0.01}$ = 2.707) and also passes the "4-to-1" rule that states the F value be at least four times larger than the critical value [25].

Table 2.3 Regression coefficients, parameters, and fit to data

Force	Regression Coefficients								Fit	
	β_0	β_1	β_2	β_3	β_4	β_5	β_6	β_7	R^2	F
F_{CH}	109.56	−2.39	0.16	−0.62	264.83	62.77	−8.30	0.31	0.98	1470
F_C	88.24	−2.20	0.15	−0.65	238.61	41.02	−6.68	0.30	0.99	2440
F_F	43.03	−1.75	0.15	−0.33	131.68	98.63	−6.59	0.37	0.91	323

Predictor Variable	*MC*	*ρ*	*VC*	*δ*
Mean Value	20.57%	544.8 kg/m^3	6.51 m/s	0.362 mm

δ_{OL} = 0.5 mm

Several significant data trends can be identified from an inspection of the regression coefficients. The signs of each coefficient and the approximate magnitudes of each coefficient were the same for each of the three response variables (forces). This indicates that the general response of each of the three forces to changes in the predictor variables was the same. Specifically, the coefficients for the moisture content and the cutting velocity main effects were negative, indicating that forces tended to decrease with increasing moisture content and cutting velocity. However, the coefficient for the density and depth-of-cut main effects were positive, indicating the reverse (forces tend to increase with increasing density and depth of cut).

2.5.2 Effect of Predictor Variables on Response Forces

To demonstrate relative and interaction effects of the predictor variables on the response variables, three cases were defined for use with the regression model and denoted as *mid-force, high-force*, and *low-force*. Each of the three cases was applied to each of the four predictor variables, one at a time. Applying the mid-force case to a predictor variable consisted of varying it from a low value to a high value and holding the other three predictor variables constant at their mean value. When moisture content was the varying predictor variable, it was varied from a low value of its mean minus one standard deviation to a high value of its mean plus one standard deviation. When density was the varying predictor variable, its range was similar with a low value of its mean minus one standard deviation and a high value of its mean plus one standard deviation. Cutting velocity, being a controlled variable, was

varied differently with a low value of the nominal minimum value included in the study (3.81 m/s) and a high value of the maximum value included in the study (9.525 m/s). Depth-of-cut was varied similarly, from its minimum nominal value (0.05 mm) to its maximum nominal value (0.65 mm).

The second case, the high-force case, also consisted of varying one of the predictor variables between the same low and high values and holding the other three predictor variables constant. However, instead of being held constant at their mean values, they were held constant at either their low value or high value depending on which increased the value of the response variable above the mid-force value. For example, when moisture content was the varying predictor variable, it was varied from its low value to its high value, density was held constant at its high value, cutting velocity constant at its low value, and depth-of-cut at its high value.

The third case, the low-force case, again consisted of varying one of the predictor variables between the same low and high values and holding the other three predictor variables constant. However, they were held constant at values that would decrease the response variables. Returning to the moisture content example, density would be held constant at its low value, cutting velocity at its high value, and depth-of-cut at its low value. To summarize, each case consists of varying one predictor variable while the others held at their mean value (mid-force case), maximum-force value (high-force case), or minimum-force value (low-force case).

Results are given in Table 2.4 for the effects of all three cases. For each case and variable combination, three parameters were calculated: the force mean ($\overline{F}$, the force magnitude corresponding to the mean value of the varying predictor variable), the force slope ($\Delta F/\Delta PV$**,** the change in force magnitude per unit change in the varying predictor variable), and the force change ($\Delta F/F$, the change in force magnitude with respect to the varying predictor variable divided by the force magnitude calculated at the low value of the varying predictor variable and expressed as a percentage).

Table 2.4 Effect of changing predictor variable magnitude

Predictor	Force	High-Force			Mid-Force			Low-Force		
		$\overline{F}$ [N]	$\frac{\Delta F}{\Delta PV}$	$\frac{\Delta F}{F}$%	$\overline{F}$ [N]	$\frac{\Delta F}{\Delta PV}$	$\frac{\Delta F}{F}$%	$\overline{F}$ [N]	$\frac{\Delta F}{\Delta PV}$	$\frac{\Delta F}{F}$%
	F_{CH}	204.4	−4.78	−12.5%	106.3	−2.29	−11.6%	23.2	0.20	5.1%
MC	F_C	171.4	−4.12	−12.9%	85.3	−2.12	−13.3%	10.3	−0.12	−6.2%
	F_F	103.8	−3.64	−18.3%	41.4	−1.67	−20.7%	0.1	0.36	231.1%
	F_{CH}	210.6	0.25	7.0%	106.3	0.16	8.8%	25.6	0.06	15.1%
ρ	F_C	176.7	0.23	7.7%	85.3	0.14	9.9%	11.5	0.05	29.9%
	F_F	107.1	0.25	14.4%	41.4	0.14	21.5%	1.8	0.03	162.0%
	F_{CH}	215.9	−0.62	−1.6%	106.3	−0.62	−3.3%	25.6	−0.62	−13.0%
V_C	F_C	181.4	−0.65	−2.0%	85.3	−0.65	−4.3%	11.9	−0.65	−27.2%
	F_F	113.3	−0.33	−1.7%	41.4	−0.33	−4.5%	2.0	−0.33	−65.2%
	F_{CH}	123.8	313.1	630%	111.1	280.5	628%	98.2	247.9	625%
δ	F_C	100.3	276.5	955%	88.3	248.9	1092%	76.4	221.3	1329%
	F_F	58.5	185.9	4047%	48.8	156.3	4985%	39.1	126.8	7547%

From the data in Table 2.4, several trends can be identified. For all cases and response variables, chain force has the largest magnitude and feed force the least, as shown by the force-mean parameter. For example, consider the high-force case of moisture content. Listed vertically, chain force exhibited the greatest magnitude of 204.4 N, cutting force a magnitude of 171.4 N, and feed force the least at 103.8 N. Interaction effects were shown by changes in the magnitude of the force-slope parameter. For example, consider cutting velocity. Reading horizontally across the table, the force-slope parameter has the same values of –0.62 for chain force, –0.65 for cutting force, and –0.33 for feed force for the high-force, mid-force, and low-force cases, indicating that no interaction exists. Additionally, the magnitude of the slope parameter was small for all forces and cases, indicating that overall, cutting velocity had a small effect on the response variables compared with the other predictor variables in the model. The moisture-content-depth-of-cut interaction and density-depth-of-cut interactions were evident from the changing values of the force slope parameter. Figure 2.10 graphically displays these interactions through

differing slopes of the regression trend line for the high-force, mid-force, and low-force cases of chain force. If no interaction existed, the slope would not change with each force case. Similar trends were observed for cutting force and feed force. The force change parameter showed that although force slope became small at the low-force condition, the change in force relative to its magnitude can be large.

Of particular interest is the moisture-content-depth-of-cut interaction. When moisture content is the varying predictor variable (*i.e.*, the rows of Table 2.4 labeled *MC*), the effect of the moisture-content-depth-of-cut interaction is shown by the force-slope parameter. For all three forces, this parameter had its greatest magnitude in the high-force case. The high force case corresponds to depth-of-cut at its maximum value. Thus, moisture content had its greatest effect on the three forces at high depths-of-cut. As the case changed from high-force to mid-force to low-force, the depth-of-cut decreased. The moisture-content-depth-of-cut interaction caused the force slope parameter to decrease in magnitude and actually become positive in the low-force case for chain force (0.20) and feed force (0.36). Thus, for all but the smallest depth-of-cut values, all three forces decreased with increasing moisture content, with the effect being greatest at high depths-of-cut (the high-force case). However, at low depths-of-cut, the trend reversed and chain force and feed force increased with increasing moisture content. This trend is shown graphically in Figure 2.10(a), where the slope of the regression trend line changes from negative in the high-force case to slightly positive in the low-force case.

(a)

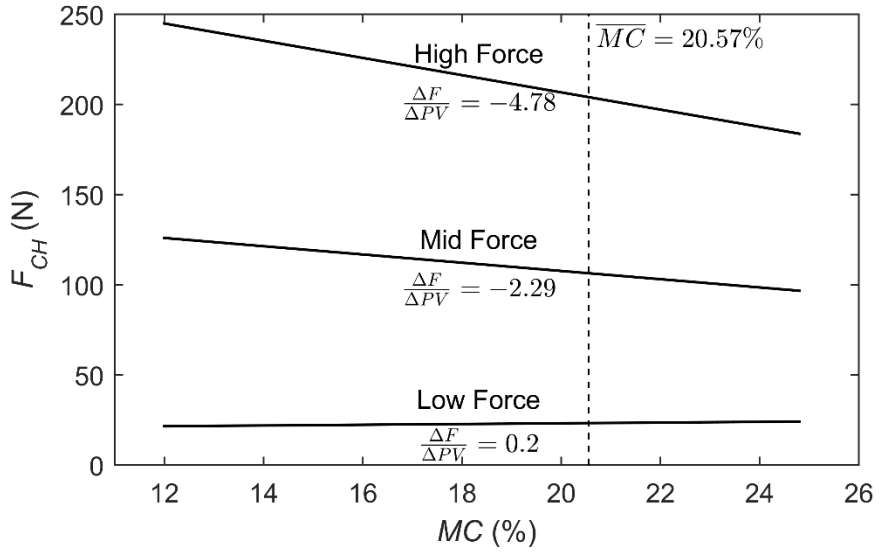

(b)

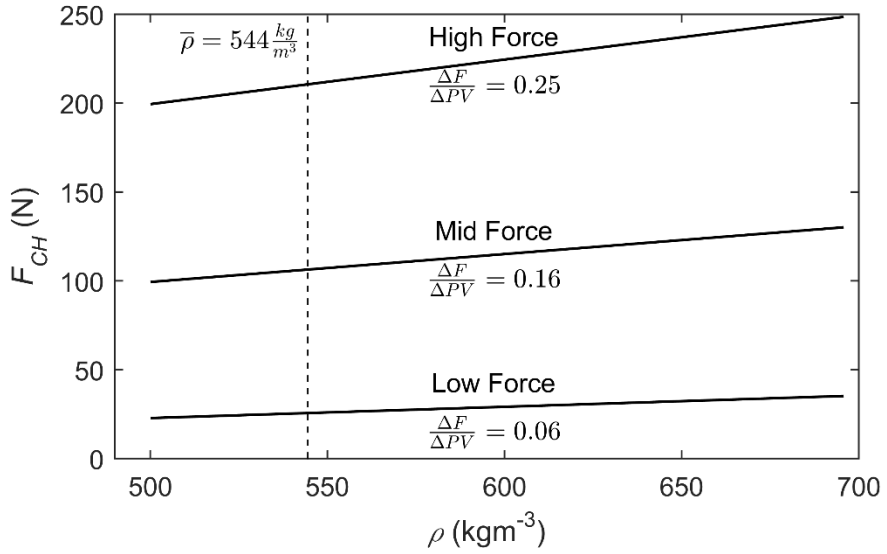

Figure 2.10 Interaction of (a) moisture content and (b) density with depth-of-cut on affecting chain force magnitude for the three force cases

This trend in the magnitude of effects with depth-of-cut has a basis in prior work. The cutting force model developed by Atkins [21] provides a theoretical foundation

for the existence of interactions in which physical properties have a reduced influence on cutting forces at low depths-of-cut. The model proposed by Atkins is the following,

$$F_C = \left(\frac{kw\gamma}{Q} + \frac{R}{Q}\right)\delta + \frac{Rw}{Q}$$

where k is the shear yield strength, w is the kerf width, γ is the shear yield strain along the primary shear band, Q is a function of friction coefficients and tool geometry, and R is the specific work of surface separation. Material-dependent parameters in the model are k and R. As can be seen, the first term in parentheses multiplying δ was controlled by material properties. Since moisture content and density can be correlated with mechanical properties [26], the first term in the Atkins cutting model is captured by the interaction terms of the regression model. Furthermore, [27] provides experimental data clearly showing that different trend line slopes are required to explain changes in cutting forces due to density at two different depth-of-cut levels. These findings support the inclusion and significance of an interaction term between physical properties and depth-of-cut in the present linear regression model.

Depth-of-cut had a significant effect on all response variables. Due to the density-depth-of-cut interaction, the greatest change in force slope occurred in the high-force case; however, unlike the effect of moisture content, this effect was uniformly positive. That is, in all cases, increased density resulted in increased cutting force, with the greatest effect at high depths-of-cut. Over the range of values of predictor variables included in the study, depth-of-cut had the greatest effect on forces. Relative effects tended to be greatest for the low-force case but were in general very large. Increasing depth-of-cut consistently and significantly increased all forces.

2.5.3 Cutting Efficiency

Cutting efficiency is a measure of the amount of cutting performed by a unit input of energy. It is a useful metric because it accounts for energetic losses that are independent of time. A high efficiency corresponds to a large amount of cutting from

a small input of energy, and a low efficiency corresponds to the reverse. Denoted by η, cutting efficiency can be calculated as

$$\eta = 1000\frac{V_F L}{F_{CH} V_C}$$

where V_F, F_{CH}, and V_C are as previously defined, and L is the length of cut (here, the length of cut is equal to the 90 mm width of the workpieces). Equivalently, substituting $V_F/V_C = \delta/PS$, cutting efficiency can also be calculated as

$$\eta = 1000\frac{\delta L}{F_{CH} PS}$$

Chain force, rather than cutting force, is used in the calculation of cutting efficiency so that losses in the drive train are included. Figure 2.11 shows cutting efficiency, chain force, cutting force, and feed force trend lines as a function of depth-of-cut, all calculated using the regression model. To capture the influence of the other predictor variables in the regression model, cutting efficiency is shown as a range of values from the high-force condition (lower solid line), mid-force condition (dashed line), and low-force condition (upper solid line). Chain force, cutting force, and feed force are all calculated at mid-force-conditions. Cutting efficiency reaches a maximum value at a depth-of-cut equal to the overload value.

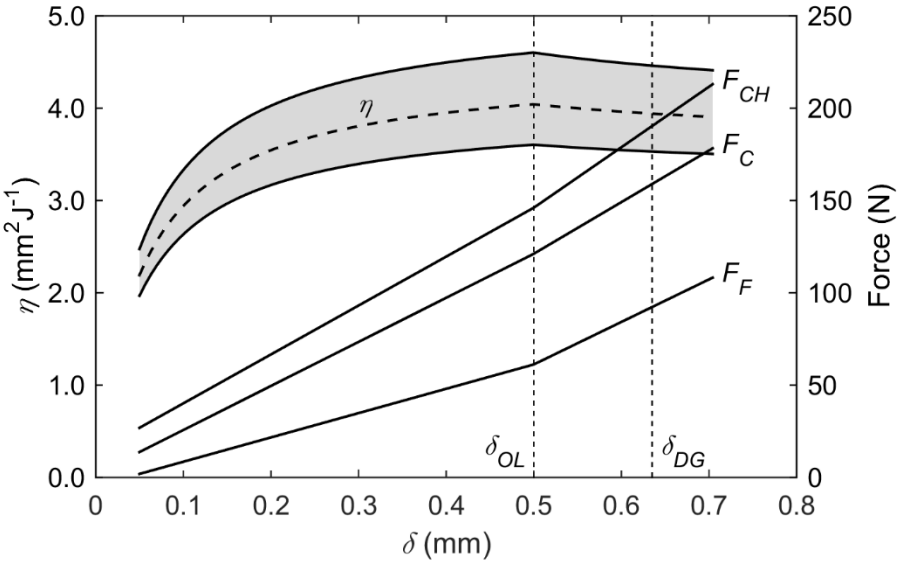

Figure 2.11 Cutting forces and cutting efficiency *versus* depth-of-cut with the overload point and depth gauge setting indicated

Given the significance of the overload value of depth-of-cut, it is worthwhile to consider what causes this and the corresponding bilinear force behavior to occur. Possible causes are the depth gauge setting and the effect of chip removal. Due to link rotation during cutting [9], the depth gauge may be pushed into the kerf bottom at depth-of-cut values less than the chain's actual depth gauge setting. Pushing the depth gauge into the kerf bottom results in increased cutting forces, both through indentation (feed force) and friction (cutting force and chain force). Also, chip removal could be a contributor due to the increase in chip size with depth-of-cut and the limited volume available in the kerf. When the available volume becomes overfilled, forces could increase at a larger rate, causing bilinear behavior.

Beneficial future work could consist of extending the range of the predictor variables included in the study. The range of moisture content and density included in the study depended on the variation in the chosen Douglas-fir dimensional timbers. While this variation was sufficient to show meaningful trends, obtaining specimens with a wider range of moisture content and density would likely show interesting results. The inclusion of greater cutting velocities, as previously discussed, would allow the exploration of a possible optimum efficiency value at high velocities.

Depth-of-cut could be further explored by varying depth gauge setting and cutter tooth geometry to investigate the causes of the overload depth-of-cut phenomena.

2.6 Conclusions

1) The change in rate of increase of cutting forces with depth-of-cut can be accurately represented by a bilinear model.

2) An optimum exists for saw-chain cutting efficiency, and it occurs at a depth-of-cut equal to the newly-termed overload value.

3) Through the inclusion of workpiece moisture content and density, an accurate regression model can be created for the prediction of saw-chain cutting forces that accounts for the inherent heterogeneity of wood mechanical properties.

4) Using this model, trends and interactions can be identified. It was shown that these trends and interactions, while newly presented for saw chains, are consistent with prior work in other types of cutting.

5) Over the range of workpiece moisture content measured in the study (12.0–24.8%), increasing moisture content was found to cause chain force, cutting force, and feed force to increase for all but the smallest depth-of-cut, with the effect being greatest at high depths-of-cut. At the smallest depth-of-cut, increasing moisture content caused chain force and feed force to increase.

6) Workpiece density, over the range measured (500–695 kg/m^3), consistently caused all forces to increase, with the greatest effect seen with high depths-of-cut.

7) Cutting velocity, varying from 3.81 to 9.525 m/s, was not found to have a large effect on any of the cutting forces.

8) Increases in depth-of-cut were found to cause chain force, cutting force, and feed force to greatly increase. This increase was found to have a bilinear behavior, with the effect of depth-of-cut being greater above a specific depth-of-cut denoted the overload depth-of-cut. In general, these trends agree with the prior research in orthogonal cutting and rigid-cutter sawing described previously in this paper.

9) For the typical saw chain, guide bar, and testing conditions of this study, optimum efficiency occurred at a feed force of nearly 60 N. This is approximately equal to the total weight of a typical battery-powered chainsaw, providing a convenient guideline for users.

10) For chainsaw manufacturers, the near independence of cutting forces with cutting velocity means that attaining optimal cutting efficiency depends primarily on the ability of the motor to supply sufficient driving torque, not power. Designing chainsaws to operate at optimum efficiency tends to extend battery life, an important consideration for cordless tools.

3 CUTTING PERFORMANCE COMPARISON OF LOW-KICKBACK SAW CHAIN

Andrew W. Otto, Levi J. Suryan, John P. Parmigiani

Pending Publication

3.1 Abstract

Kickback is the leading cause of the most severe and traumatic chainsaw related injuries. As a result, safety standards require chainsaw manufacturers to produce low-kickback saw chain. In order to understand the tradeoffs in current state of the art saw chain, a comparison study was conducted on a custom test apparatus using four different saw chains, all with the same cutter geometry but different low-kickback chain features. Two modes of cutting were studied: nose-clear down bucking and boring. Cutting performance for boring with a chainsaw has not been studied previously. Regression modelling was used to generate cutting force and cutting efficiency trend lines for each of the different saw chains and cutting modes. In nose-clear down bucking, it was found that operator effort and cutting efficiency of a low-kickback chain with bumper drive links was of near-equal performance to that of a non-low-kickback chain (having no low-kickback features). In boring, all types of low-kickback saw chain elements required markedly higher operator effort and had lower cutting efficiency that of non-low-kickback saw chain. Furthermore, a substantial difference in cutting forces was found between differing designs of bumper drive link elements in both nose-clear down bucking and boring, highlighting the importance of proper bumper link geometry. Using these results and considering that the boring mode of operation is for experienced users, the casual chainsaw operator should always prioritize safety by using a low-kickback saw chain while professional users should select the chain that best suits their current cutting needs.

3.2 Introduction

Chainsaws are inherently dangerous to operate [28–31]. The most severe and traumatic chainsaw related injuries—typically to the head and neck—are caused by chainsaw kickback [29,30,32]. Chainsaw kickback is the rapid motion of the guide bar towards the user [33,34]. The motion can be rotational or translational but the former is more common, more dangerous, and will exclusively be the focus of this paper. Rotational kickback occurs when the saw chain passing over the upper quadrant of the guide-bar tip (i.e. the end of the guide bar not attached to the chainsaw

power head) contacts the workpiece, cuts too deeply, and comes to an abrupt stop [33,34]. Momentum is then transferred from the saw chain causing a rapid rotation, often exceeding 1000 deg/s, of the guide bar towards the user [35].

The danger associated with kickback has led to means for its prevention being included in the American National Standards Institute (ANSI) standard B175.1. This standard includes kickback-prevention design criteria that chain saw manufacturers must satisfy. These criteria include a requirement that chainsaws have "features to reduce the risk of injury from kickback". The standard allows manufacturers some discretion in selection; however, features typically implemented on commercial chain saws are reduced kickback guide bars, chain brakes, and low-kickback saw chain. Reduced kickback guide bars provide less area for kickback-inducing contact to occur by having specially-designed smaller-radius tips. Chain brakes quickly stop motion of the saw chain about the guide bar when kickback occurs, thus greatly reducing the potential for injury if contact with the operator occurs. Low-kickback saw chain inhibits overly deep cuts through modifications to cutter and link geometry.

Of these commonly-used means of reducing the risk of kickback, only low-kickback saw chain, due to limiting depth-of-cut, directly affects cutting effectiveness and efficiency. This has led to significant research and development efforts resulting in the commercial offering of many varieties of low-kickback saw chain designed to also cut well. These designs originated from patents describing special guard links in the saw chain to prevent jamming due to sticks and debris [36,37]. Adaptations of these guard links were then used to limit engagement of cutter teeth as they traversed the nose of the guide bar [38–40]. Through largely unpublished proprietary research, manufacturers continue to develop low-kickback saw chain to improve its cutting performance [41,42].

Evaluating the cutting performance of all types of saw chain is also a significant area of research, some of which has been published. Work with individual saw chain links has quantified the influence of cutter geometry and orientation on cutting forces [3,4,9]. Other research has used complete saw chains. McKenzie [2] compared the performance of (at the time) newer saw chain designs to older

"scratcher" type, while also developing useful metrics for evaluating the cutting performance of saw chain. Experiments by Reynolds [7] revealed a linear relationship between cutting forces and depth-of-cut for saw chains. Stacke [9] developed a full dynamic model for the saw chain during cutting using force data taken from single cutter experiments, and found similar linear relationships between depth-of-cut and cutting forces that was independent of chain velocity. Otto and Parmigiani [43] used regression modelling to average the influence of wood physical properties on cutting force measurement, permitting comparison of chains across large numbers of wood specimens of the same species. Their work also showed that chains exhibit a peak cutting efficiency based on an overload depth-of-cut parameter.

Missing in the published literature is a scientific comparison of the cutting performance of low-kickback saw chain. To what extent is the performance of low-kickback saw chain reduced as compared to non-low-kickback saw chain (referred to hereafter as professional saw chain)? What tradeoffs exist when using a low-kickback saw chain? How do the various depth-of-cut limiting features used to create low-kickback saw chain affect cutting performance? This paper contributes to answering these questions by presenting a scientific study of the cutting performance of several modifications made to standard saw chain to create low-kickback saw chain. Specifically, this study compares four saw chains with identical cutting tooth geometries with different low-kickback elements. Data is generated using a custom saw-chain testing machine. Both nose-clear down-bucking (downward cuts not using the tip of the guide bar) and boring (plunge cuts using the tip of the guide bar) are included in the study. Results identify the differences in the performance of professional and low-kickback saw chains, as well as which cutting operations are most impacted by the use of a low-kickback saw chain.

3.3 Materials and Methods

3.3.1 Saw Chain

Saw chain can be classified as either professional or low-kickback. The key elements of a typical professional saw chain are illustrated in Figure 3.1(a) showing drive links, cutter links, and tie straps. Drive links engage a drive sprocket which propels the saw chain about the periphery of the guide bar. Cutter links consist of a

chisel cutter and a depth gauge. The chisel cutter performs the actual wood cutting and the depth gauge limits its depth-of-cut. On professional chain, the depth gauge is the only feature that specifically controls depth-of-cut. The key elements of typical low-kickback saw chain are illustrated in Figure 3.1(b) and Figure 3.1(c). The former shows a modified tie strap, referred to as a *bumper tie strap*, which is elevated and inclined to correspond to the depth gauge. Similarly, the latter shows a modified drive link, referred to as a *bumper drive link,* which also has an elevated and inclined section corresponding to the depth gauge. Both bumper tie straps and bumper drive links supplement the depth gauge in controlling depth-of-cut.

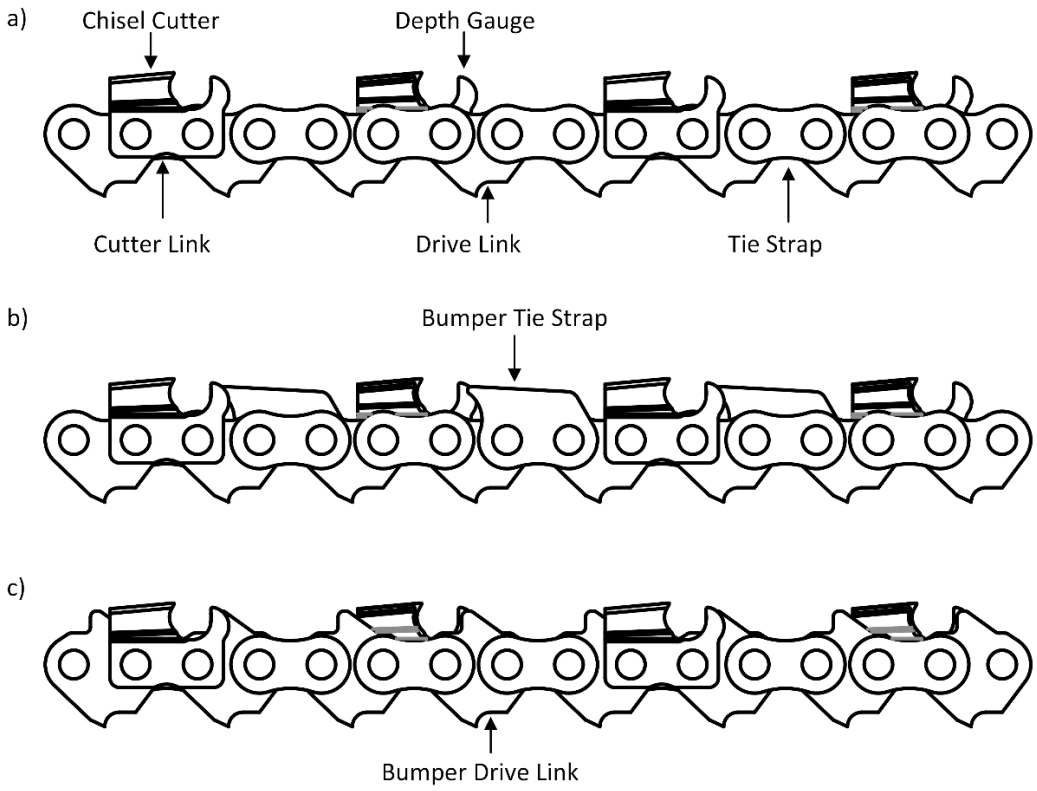

Figure 3.1 Saw chain terminology and low-kickback saw chain elements (a) professional, non-low-kickback chain, (b) bumper tie strap low-kickback chain, (c) dumper drive link low-kickback chain

The need for supplemental control of depth-of-cut is illustrated in Figure 3.2 showing a section of professional chain traversing the free end of a guide bar. Note the large difference in the depth-of-cut allowed by the depth gauge for a (down) bucking cut *versus* a boring cut. When the saw chain is traversing the upper or lower

surfaces of the guide bar, as during bucking cutting, the chain links are aligned and the depth gauge is effective in limiting the depth-of-cut of the cutter link to relatively small values. However, when the saw chain is traversing the nose of the guide bar, as during boring or other cutting involving the bar tip, the links are not aligned and the depth gauge is much less effective and allows a large depth-of-cut which can lead to chainsaw kickback. Bumper tie straps and bumper drive links are specifically designed to limit depth-of-cut when the saw chain is traversing the nose of the guide bar by articulating relative to the cutter link.

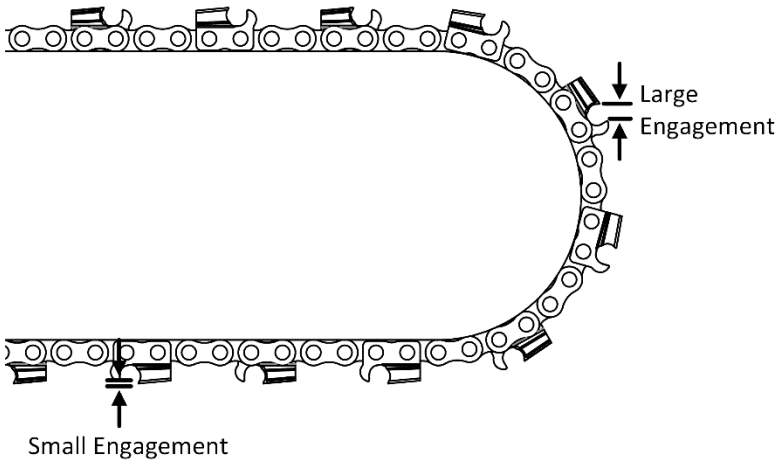

Figure 3.2 Increase in depth-of-cut as cutter links traverse the guide bar nose

Four saw chains were selected for this study. All four chains had the same cutter link geometry. The only difference between each chain was the low-kickback feature present. Each chain was in the new, out-of-box condition. The first chain, denoted *Chain A*, was professional chain and contained no low-kickback features and is thus referred to as the *naked specimen*. The second, denoted as *Chain B*, featured bumper tie straps meeting the ANSI B175.1 standard and is referred to as the *bumper tie strap specimen*. The third and fourth, denoted to as *Chain C* and *Chain D* respectively, both contain bumper drive links. Chain C and Chain D have a slight difference in the geometry of their bumper drive links and are included in the study to highlight the influence of chain-link geometry on cutting performance. Specifically, Chain C has a larger ramped portion on the top of the drive link compared to Chain D. They are referred to respectively as the *Bumper Drive Link – 1 specimen*

and the *Bumper Drive Link – 2 specimen*. The same guide bar and six-tooth spur sprocket were used for all chains throughout testing.

3.3.2 Measured and Calculated Parameters

The same measured cutting parameters used in previous work [43] are adopted for the current work, along with the boring cutting mode of operation. Classically, cutting experiments with saw chain have been performed in the nose-clear down bucking mode, where the guide bar is fed vertically downward into a workpiece with the nose of the guide bar being clear of material. In this work, testing is also conducted in the boring mode of operation, where the nose of the guide bar is plunged horizontally into the workpiece and fed until the nose exits the opposite side of the workpiece. In nose-clear down bucking, the cutting force (F_C) and feed force (F_F) are the measured reaction forces on the workpiece in the horizontal and vertical directions, respectively. This convention flipped for boring, as displayed in Figure 3.3 where the cutting force and feed force are the reaction forces on the workpiece in the vertical and horizontal directions, respectively. The saw chain is propelled by the drive sprocket with drive torque T_M and angular velocity ω. The reaction force on the bar due to chain tension is denoted F_T. The feed velocity is denoted V_F, which is always in the direction of the feed force and the motion of the body of the saw.

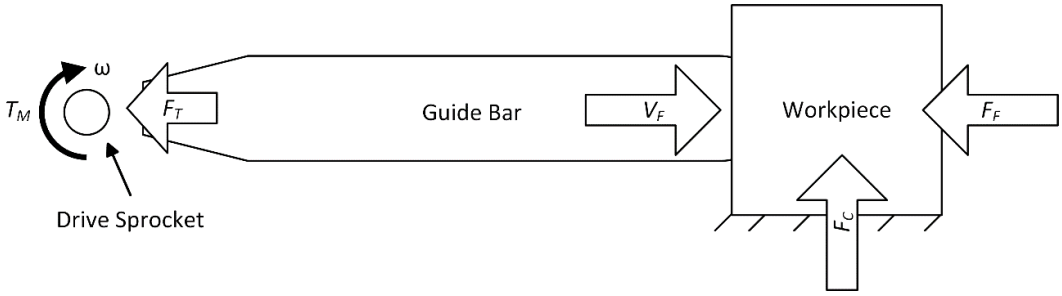

Figure 3.3 A diagram of a chainsaw performing a boring cut showing the measured cutting parameters of drive torque and velocity, chain tension, feed force and velocity, and cutting force

Three quantities are calculated from the parameters defined in Figure 3.3, with equations listed in Table 3.1. The chain force (F_{CH}) is the effective tangential force applied by the motor torque to drive the chain through the wood during cutting.

Chain velocity (V_C) is the speed of the chain as it moves around the periphery of the bar and is a function of the drive sprocket velocity. Depth-of-cut is the theoretical chip thickness cut by each pair of left- and right-handed cutter pairs and depends upon chain velocity, feed velocity, chain pitch (P), and chain spacing (S) [43].

Table 3.1 Calculated cutting parameters

Parameter	Calculation
Chain Force (N)	$F_{CH} = T_M \left(\frac{\pi}{(1000P)n}\right)$
Chain Velocity (m/s)	$V_C = \frac{\omega}{2\pi} 2(1000P)n$
Depth-of-cut (mm)	$\delta = \frac{V_F}{V_C} P\ S$

3.3.3 Test Apparatus

The test apparatus used in this work was developed previously and accurately measures the parameters described above under rate-controlled conditions [43]. The apparatus uses standard off-the-shelf guide bars and drive sprockets. Three subsystems make up the mechanical portion of the machine: the power head, which drives the chain with an AC motor; the work holding system, which measures reaction forces and restrains the workpiece; and the motion system, which has two linear axes of motion and controls the cutting rate. An overall view of the machine, with labeled subsystems, is shown in Figure 3.4. Motor drive torque (T_M), chain tension (F_T), cutting force (F_C), and feed force (F_F) are recorded during cutting at 2 kS/s using industry standard strain-gage based torque and force transducers and a National Instruments CompactRIO data acquisition system running LabVIEW. A 200-point moving average filter was used to reduce mechanical noise present in the measured torque and force waveforms.

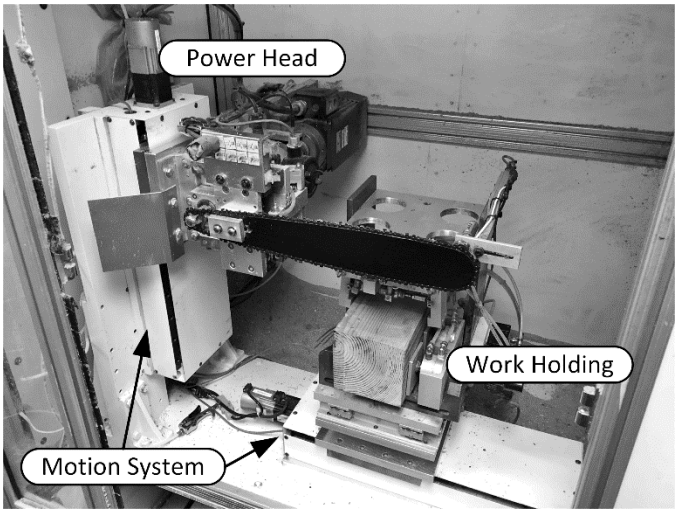

Figure 3.4 Testing machine used to measure cutting forces and control cutting rates during experiments

3.3.4 Test Media

Workpieces for testing were obtained from Douglas-fir dimensional timbers 3.0 m in length with rectangular cross section (90 by 140 mm). They were hand selected from a local lumber supplier such that grains were oriented vertically in nose-clear down bucking and horizontally in boring to allow the chain to instantaneously pass through equal amounts of early- and late-wood while cutting. The end-grain orientations for each mode are displayed in Figure 3.5. The number of knots was minimal. Each timber was divided into four 25 cm long workpieces, sized to fit in the safety enclosure of the testing machine. Cuts were equally spaced in each workpiece to produce offcuts of approximately 20 mm in thickness.

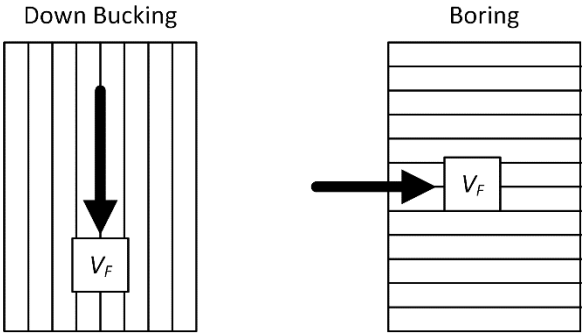

Figure 3.5 End-grain orientations for down bucking and boring cutting modes

3.3.5 Test Procedure

Each cut performed with the test apparatus followed the same procedure, which is similar to that used in previous testing with the same machine [43]. First, the guide bar and one of the four chains for testing were installed on the power head. Then, the workpiece corresponding to the current randomized experimental run was inserted into the work holding system. Next, the power head was turned on at the desired chain speed to take an average measurement of the non-cutting chain tension for two seconds. If the chain tension was above or below the specified control point for any test by more than 5 N, the machine would request adjustment by the operator. Adjustment, if necessary, was performed using the tensioner screw located on the bar mount of the power head. Once the chain tension was within tolerance, the machine would again start the power head at the desired chain velocity, dwell for 1 second, weigh the workpiece, and perform the cut at the desired feed rate while recording force and torque values. Following the cut, the machine would return to its starting position and automatically load the chain velocity and feed rate for the next cut, awaiting operator input to start the next cut. All cuts were performed with bar lubricating oil applied at a manufacturer recommended 5 mL/min through the standard oiling orifice of the guide bar.

Immediately after cutting, each offcut was collected for measurement of moisture content and density. Moisture content was measured using a Delmhorst J-200 moisture content meter by inserting the measuring probes into the center of the wood cross section. Density was calculated from the measured mass and volume of the offcut. Mass was measured with a gram scale and offcut volume (length × width × height) was measured using digital machinist's calipers.

3.3.6 Data Processing

Several post processing steps were necessary before using the collected data for regression modeling, and are largely identical to those used in earlier work with the same experimental setup [43]. First, the raw torque and force values were passed through a 200-point moving average filter to remove noise. Workpiece weight was subtracted from the measured vertical reaction force during cutting. Motor drive

torque was converted into chain force (F_{CH}). These steps result in the cutting force waveforms shown in Figure 3.6(a). For regression modeling, a singular measured value is required from each cut that represents the cutting force. To achieve this, an effective average is obtained by placing each force channel into 15 equally spaced bins of a histogram, and picking the center point of the bin with the highest frequency of samples as the representative force value, which is displayed in Figure 3.6(b). Past work has shown this method to be effective in reducing the influence of knotty samples on skewing cutting data, allowing the inclusion of cuts with knots present in the regression model [43].

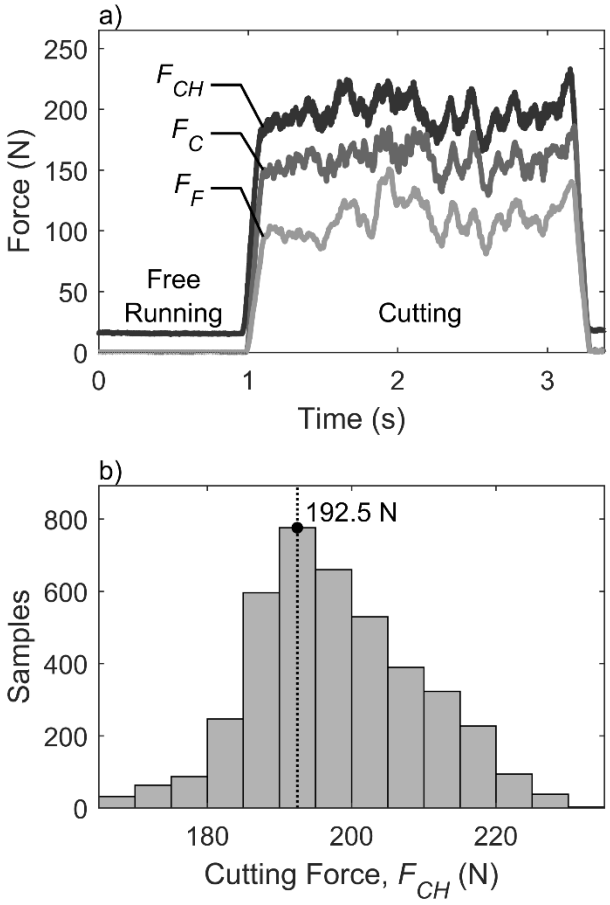

Figure 3.6 (a) Representative cutting force waveform collected during a single cut, (b) the histogram method used to extract the effective cutting force (192.5 N in this case) from the force waveforms

3.3.7 Data Analysis

Multiple linear regression was used for analyzing the raw cutting data and generating trends for each test. The measured chain force, cutting force, and feed force served as responses for linear regression. Three predictors were used: the controlled variable depth-of-cut (specified) and the uncontrolled variables moisture content and density (measured). Prior work has shown that tracking workpiece properties allows for reduction of the influence wood heterogeneity has on the cutting force data [43]. Furthermore, including workpiece properties in the regression models permits comparisons between different chain designs even though the separate tests did not all cut in the exact same test media. Chain velocity was held fixed at 7.62 m/s (4000 RPM on a 6-tooth sprocket) for all testing, as prior work has shown cutting velocity has little effect on cutting forces in the velocity envelope of the testing machine, which is approximately 1500–7000 RPM [43].

The regression model used has all main effects as well as the interactions of moisture content and density with depth-of-cut. This model was selected based on its adequacy in preceding tests with similar chains and test media, with the only difference being the omission of chain velocity as a predictor variable [43]. The model equation used for down bucking is of the form

$$F_{CH},\ F_C,\ F_F = \beta_0 + \beta_1(MC^*) + \beta_2(\rho^*) + \beta_3(\delta^*) + \beta_4\langle\delta - \delta_{OL}\rangle + \beta_5(MC^*)(\delta^*) + \beta_6(\rho^*)(\delta^*)$$

where

$$\langle\delta - \delta_{OL}\rangle = \begin{cases} 0 \text{ if } \delta^* \le \delta_{OL} - \bar{\delta} \\ \delta - \delta_{OL} \text{ if } \delta^* > \delta_{OL} - \bar{\delta} \end{cases}$$

In the preceding equation, *MC* refers to moisture content, ρ is wood density, δ is the depth-of-cut, and δ_{OL} is the overload depth-of-cut, as defined by [43], and is used for bilinear regression in depth-of-cut. Variables with an asterisk superscript (*i.e.* MC^*) have been centered about their mean value for samples within that particular subset of chain's data. For example, $\rho^* = \rho - \bar{\rho}$, where the overbar notation denotes the mean value of a given predictor variable for one of the four chains.

The model equation used for boring cuts is of the form

$$F_{CH},\ F_C,\ F_F = \beta_0 + \beta_1(MC^*) + \beta_2(\rho^*) + \beta_3(\delta^*) + \beta_4(MC^*)(\delta^*) + \beta_5(\rho^*)(\delta^*)$$

where the only difference from down bucking is the omission of the overload depth-of-cut term (δ_{OL}), as large depths of cut are generally not attainable in the boring cutting mode.

3.4 Results

3.4.1 Collected Data and Regression Model

Testing consisted of making repeated cuts with each chain at varying depths of cut and fixed chain speed (7.62 m/s). Seven depth-of-cut levels (0.05, 0.15, 0.25, 0.35, 0.45, 0.55 and 0.65 mm) were used for each chain in the down bucking cutting mode, while five levels (0.05, 0.0875, 0.125, 0.1625, and 0.2 mm) for each chain were used in the boring cutting mode. Eight replicates of each depth-of-cut level for each of the four saw chains resulted with a total of 224 cuts (56 cuts for each chain) in down bucking and 160 cuts (40 cuts for each chain) in boring. These cuts were dispersed between the workpieces, with 4 replicates in each workpiece. Cuts were randomized within workpieces to reduce systematic error.

Before forming the regression models, the raw data for the workpiece properties of moisture content and density was studied. Average values and standard deviations of workpiece properties with respect to each chain tested are displayed in Table 3.2. Overall, moisture content varied from 10.1% to 26.8% and density from 452 to 733 kg/m^3. The large range in density is attributed to the few offcuts with knots present. Low moisture content levels were only present in a small number of cuts that occurred near the open ends of the timbers due to air drying during storage at room temperature. Within each cutting mode, the distribution of wood material properties was consistent across each chain, which enables cross-comparison of the regression model results when the physical properties are treated as random variables.

Table 3.2 Measured workpiece moisture content and density

Cutting Mode	**Chain**	***MC* (%)**		***ρ* (kg/m^3)**	
		Mean	Standard Deviation	Mean	Standard Deviation
Down Bucking	A	23.9	2.8	491	24.6
	B	24.7	0.6	498	27.4
	C	24.8	0.6	531	62.6
	D	24.9	0.6	512	54.9
	Total	24.6	1.6	508	46.6
Boring	A	23.6	2.1	555	24.9
	B	21.0	3.7	537	47.2
	C	23.6	2.4	547	18.7
	D	23.7	1.5	548	23.6
	Total	22.8	3.0	547	31.1

Regression coefficients and model fitment summary, quantified by the coefficient of determination (R^2) and F-statistic, are provided in Table 3.3 for the down bucking experiment and in Table 3.4 for the boring experiment. Overall, good fitment was obtained as indicated by high R^2 values and statistically significant regression with F-values much greater than the critical F-value for the experiments ($F_{6,49,0.05}$ = 2.29 for down bucking and $F_{5,34,0.05}$ = 2.49 for boring). Lower R^2 values were obtained for the boring cutting experiment which is attributed to covering a smaller range in depth-of-cut compared to the down bucking experiment.

Table 3.3 Regression model coefficients and fit, down bucking

Chain	Force	Regression Coefficients							Fit	
		β_0	β_1	β_2	β_3	β_4	β_5	β_6	R^2	F
A	F_{CH}	103.36	–0.91	0.02	239.83	84.54	–3.01	0.46	0.99	690
	F_C	80.92	–0.82	–0.09	224.72	50.33	–4.21	0.01	0.98	339
	F_F	31.73	–0.05	–0.05	90.97	104.82	0.87	–0.16	0.98	407
B	F_{CH}	108.93	–3.54	0.03	256.14	75.51	–16.89	–0.26	0.99	880
	F_C	79.39	1.31	–0.03	227.93	63.71	–10.03	–0.12	0.99	1080
	F_F	37.69	1.71	–0.01	120.09	198.16	–4.08	–0.12	0.99	574
C	F_{CH}	106.18	7.15	0.13	272.53	84.59	16.68	0.40	0.99	766
	F_C	78.24	8.59	0.12	228.40	114.95	16.74	0.47	0.99	565
	F_F	41.84	6.33	0.08	138.86	215.30	30.34	0.26	0.96	168
D	F_{CH}	105.40	2.33	0.10	247.48	32.77	7.04	0.17	0.99	782
	F_C	77.42	1.60	0.08	212.82	43.50	–3.32	0.13	0.99	712
	F_F	31.63	4.96	–0.01	89.53	99.18	23.77	–0.09	0.98	320

Table 3.4 Regression model coefficients and fit, boring

Chain	Force	Regression Coefficients						Fit	
		β_0	β_1	β_2	β_3	β_4	β_5	R^2	F
A	F_{CH}	82.46	–1.62	0.14	239.77	–4.98	1.14	0.95	123
	F_C	79.61	–0.20	0.02	120.05	6.05	0.58	0.75	21
	F_F	41.58	–1.14	0.07	106.46	–5.77	0.41	0.90	60
B	F_{CH}	93.81	–1.29	0.12	290.69	–4.04	0.57	0.95	128
	F_C	108.40	–1.24	0.05	273.07	–3.54	1.61	0.84	36
	F_F	57.30	–1.97	0.20	160.49	–6.85	0.85	0.87	45
C	F_{CH}	95.78	–3.43	0.23	276.00	–11.91	1.84	0.87	38
	F_C	119.43	–2.70	0.24	303.37	16.10	3.53	0.85	32
	F_F	46.77	–2.64	0.18	146.09	–18.86	0.30	0.85	31
D	F_{CH}	85.77	–1.42	0.17	249.91	–5.70	1.51	0.97	221
	F_C	89.69	1.52	0.17	164.03	–0.02	0.94	0.87	44
	F_F	39.27	–2.60	0.04	122.53	–5.47	0.23	0.93	89

For down bucking, each chain required different values of the overload depth-of-cut for the regression models shown in Table 3.3. The overload depth-of-cut values used in the regressions were selected by forming the root mean square error (RMSE) of feed force as a function of overload depth-of-cut, which is displayed in Figure 3.7. Feed force was used over the other responses as it proved most sensitive to this fitting parameter. Minimizing the RMSE of feed force as a function of overload depth-of-cut enabled objective selection of an overload depth-of-cut value that accurately captures the bilinear-overload behavior of saw chain, as shown in related work, provided a global minimum exists [43].

Regressions for feed force were formed for 100 linearly spaced overload depth-of-cut values between 0.1 and 0.6 mm to generate the RMSE *versus* overload depth-of-cut function in Figure 3.7. Resultant minimums and their respective feed force RMSE values are reported in Table 3.5. As can be seen, all chains' feed force RMSE displayed a definite, unique minimum. Chain D had the lowest overload depth-of-cut at 0.29 mm while Chain B had the highest at 0.49 mm. Chains A and C had very similar overload depth-of-cut values of 0.39 mm and 0.38 mm, respectively. Chain C had the largest feed force RMSE of 9.34 N, while the other three chains were all grouped in the 4–5 N zone.

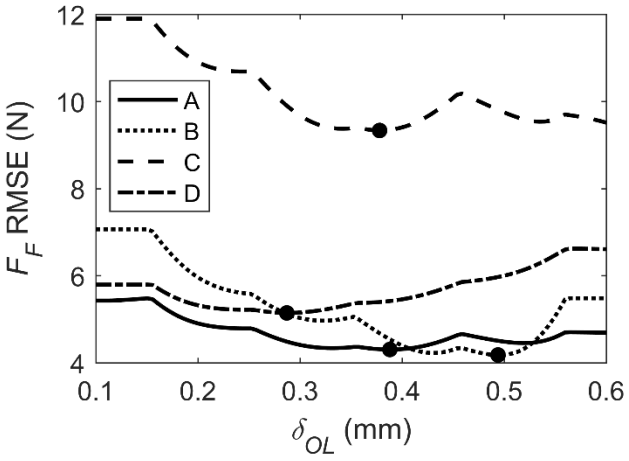

Figure 3.7 Root mean square error (RMSE) of feed force (F_F) as a function of overload depth of cut (δ_{OL}) for each chain used in the low-kickback study in down bucking. Minimums are indicated using solid dots on each line

Table 3.5 Selected overload depth-of-cut values, down bucking

Chain	δ_{OL} (mm)	F_F RMSE (N)
A	0.39	4.30
B	0.49	4.18
C	0.38	9.34
D	0.29	5.15

3.4.2 Cutting Forces and Cutting Efficiency Comparison

Using the regression coefficients in Table 3.3 and Table 3.4, trend lines were calculated for chain force, cutting force, and feed force *versus* depth-of-cut for both the down bucking and boring modes. A fourth group of trend lines was formed by calculating the cutting efficiency (η) from chain force, as defined by [43], and plotting *versus* depth-of-cut. All trend lines are shown in Figure 3.8. The influence of moisture content and density was factored out of the trend lines by using the total averages for both moisture content and density listed in Table 3.2 for down bucking and boring.

For down bucking, the four chains performed similarly with respect to chain force, cutting force, and cutting efficiency as indicated by the tight proximity of the trend lines and peak values in Figure 3.8. Feed force (F_F) showed the largest differences between chains. The peak feed force values for Chains A–D were 85, 104, 137 and 90 N, respectively. The “knee” in each of the trend lines is due to the presence of the overload depth-of-cut parameter in the regression model for down bucking.

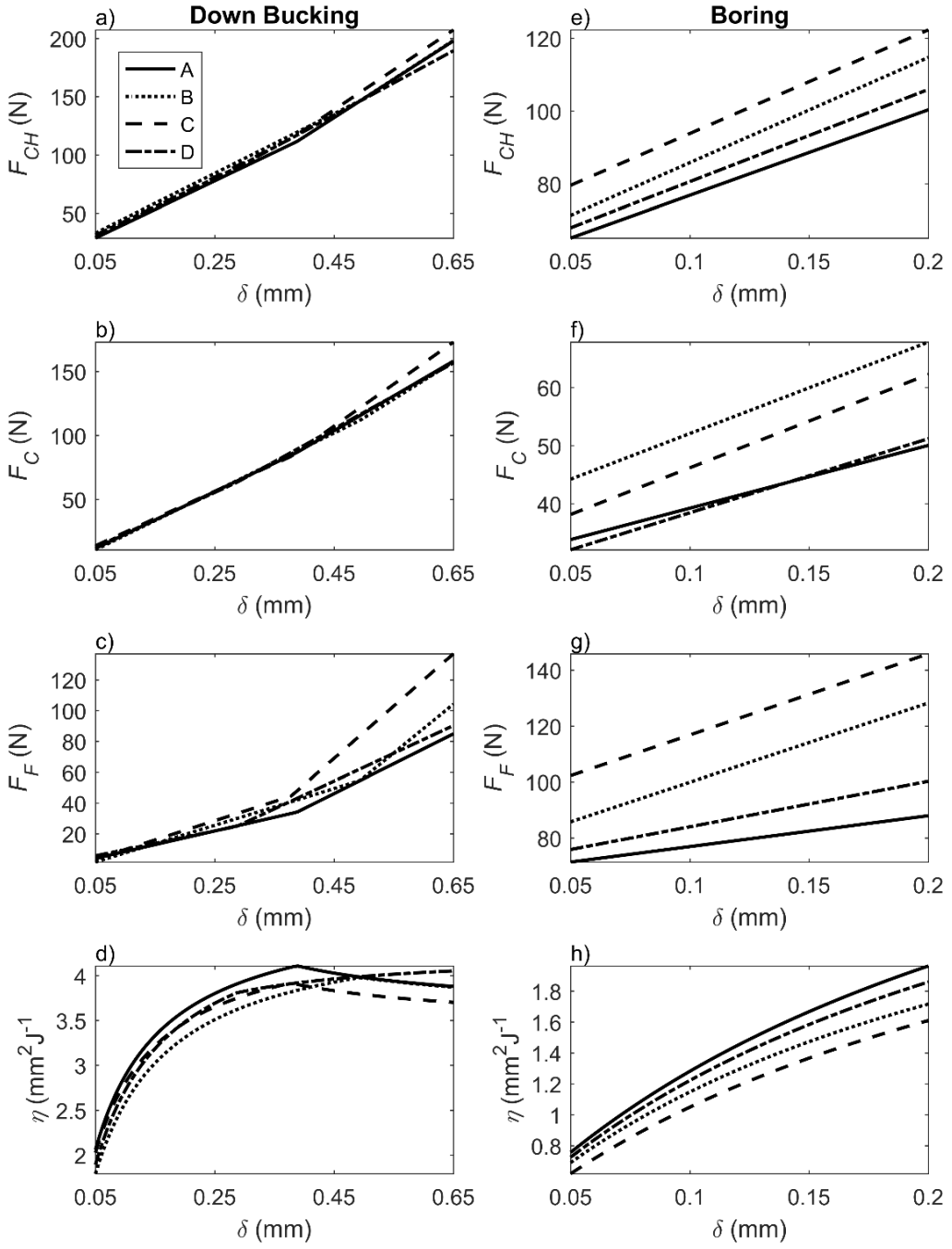

Figure 3.8 Chain force (F_{CH}), cutting force (F_C), feed force (F_F), and cutting efficiency (η) plotted *versus* depth of cut (δ) for each of the four chains (A, B, C, D) used in the low-kickback comparison study for both the down bucking (left column, a–d) and boring (right column, e–h) cutting modes

In boring, straight line fits were obtained for each force trend line *versus* depth-of-cut due to the absence of the overload depth-of-cut parameter from the regression model. The chain force (F_{CH}) trend lines are largely parallel, with Chain A (naked) exhibiting the lowest peak chain force of 100 N and Chain C (bumper drive links) having the highest peak chain force of 122 N. Again, feed force had the largest differences between chains with peak values of 88, 128, 145, and 100 N for Chains A–D, respectively. In cutting efficiency, Chain A was the best performer with a peak of 1.96 mm^2/J, while Chain C had the lowest efficiency with a peak of 1.61 mm^2/J. Overall, Figure 3.8 clearly shows that the Chain A had the lowest cutting forces as well as the highest efficiency in the boring cutting mode. Furthermore, Chain D (bumper drive links) closely follows the cutting performance of Chain A while meeting the ANSI low-kickback standard.

3.5 Discussion

The similarity in forces for down bucking in the cutting direction (F_{CH} and F_C) between chains in Figure 3.8(a–b) is attributed to each chain having the same cutter link geometry. This similarity in forces is expected since the different low-kickback elements primarily work in the direction that opposes the feed direction of the chain (perpendicular to the cutting direction), hence having minimal effect on the cutting forces. On the other hand, differences in feed force among chains for down bucking (Figure 3.8(c)) as well as all forces for boring (Figure 3.8(e–h)) are attributed to the different low-kickback elements between each chain working in opposition of the feed direction.

Ideally, a saw chain cuts with the least force input from the operator. In other words, a high-performing saw chain should cut with large depth of cut under typical feed forces. Thus, a high-performing saw chain would cut with greater speed than a lower-performing chain under the same feed force input from the operator. Typical feed forces in down bucking are close to the weight of the saw itself, which is roughly 50 N. Inspecting Figure 3.8(c) and reading the depth-of-cut for each chain at 50 N ranks the chains in terms of cutting speed, with the best-to worst ranking for down bucking being Chain A-B-D-C. Interestingly, the y-intercepts on the feed force plot for down bucking of Figure 3.8(c) are nearly identical across all four

chains, which indicates the slope of the trend line controls the cutting rate along with the “knee” in the trend line due to the overload depth-of-cut. Therefore, feed force vs. depth-of-cut slope (N/mm) and overload depth-of-cut (mm) are useful descriptors of the cutting performance for a chain in the down bucking cutting mode. In the boring cutting mode, the performance differences between chains can be clearly seen from the feed force in Figure 3.8(g). The best-to-worst ranking in terms of boring feed force is Chain A-D-B-C.

Another interesting result from the experiment comes from comparing Chain C and Chain D (bumper drive links). The only feature separating these chains is a slight difference in the bumper drive link shape. Despite this small difference, the variation in cutting forces between these two chains is considerable in both down bucking and boring. Chain C was the overall worst-performing low-kickback saw chain while Chain D was the overall best performing. The large performance difference highlights the sensitivity of low-kickback link geometry to cutting forces and the importance of careful low-kickback link design.

In the general case, cutting performance differences between a *properly designed* low-kickback saw chain and the non-low-kickback version are small under *most* operating conditions. Therefore, the present experimental results support the notion that saw chain meeting the ANSI B175.1 low-kickback saw chain standard should be used for the large majority of chainsaw operations for improved safety. Certainly, low-kickback saw chain will not perform boring cuts as easily as a non-low-kickback saw chain since that is precisely the type of cutting the bumper links act to prevent. It is the intent of the authors that this study provides useful quantitative information on the performance differences between low-kickback and professional saw chain such that consumers and professionals alike can always prioritize safety depending on the type of cutting being performed.

3.6 Conclusions

The cutting performance of three low-kickback saw chains and one professional saw chain was compared under controlled cutting conditions in down-bucking and

boring cutting modes. Under all cutting conditions, professional saw chain exhibited the lowest cutting forces and therefore the highest cutting efficiencies. For typical depth-of-cut values, the performance advantage of a professional saw chain in down bucking was marginal compared to the best-performing low-kickback saw chain, which used bumper drive links. Feed force, an indicator of operator effort during cutting, was the most sensitive response to changes in low-kickback saw chain elements. Large differences in feed force between the professional chain and low-kickback chains were observed in the boring cutting mode. Additionally, each chain required different overload depth-of-cut values in the regression model despite having the same cutter link geometry, indicating the safety elements control depth-of-cut and the onset of overload during cutting. Therefore, overload depth-of-cut can serve as a useful parameter for comparing different chains.

The data presented for testing in the boring cutting mode under controlled conditions is new to the chain saw cutting literature. In addition, this study provides a method for determining a saw chain's overload depth-of-cut using regression methods. For general use, the authors recommend low-kickback rated saw chain for two reasons: (1) chain saws are most commonly operated in nose-clear down bucking conditions, and (2) the measured cutting performance differences in this study are small under down bucking conditions.

The results of this study highlight the sensitivity of cutting performance to the geometry of the low-kickback links on saw chain. Investigation into the influence of low-kickback link geometry on cutting performance would be a useful extension of the present work. One of the main challenges in low-kickback link design is parameterizing the shape in such a way to enable controlled design iteration—essentially establishing the dependence of cutting forces on link shape.

4 CONCLUSION

A custom test stand for saw chain was built to measure cutting forces and cutting efficiency. Multiple linear regression was used to generate predictive models for cutting forces accounting for depth-of-cut, overload depth-of-cut, workpiece moisture content, workpiece density, and interactions between depth-of-cut with moisture content and density. The modeling choices captured workpiece variations by treating moisture content and density as random, uncontrolled variables. A bilinear model with respect to depth-of-cut was necessary to express the overload phenomenon observed when cutting in the down-bucking mode. In general, cutting forces were most strongly controlled by depth-of-cut, and increased proportionally with depth-of-cut. Cutting forces were shown to decrease with increasing moisture content and increase with increasing density; a trend that is consistent with existing wood cutting literature. Chain velocity had a negligible effect on cutting forces and cutting efficiency over the range tested. Additionally, the regression models showed interactions between depth-of-cut and physical properties that are new to the chainsaw cutting literature—namely that moisture content and density had a reduced influence at small depths-of-cut and increased influence at large depths-of-cut.

Using the established test methods, four chains with identical cutter links—one non-low-kickback chain and three different low-kickback chains—were compared in both nose-clear down bucking and boring. The results show that the best performing low-kickback saw chain had marginal differences in operator effort (*i.e.* feed force) and cutting efficiency compared to a professional non-low-kickback saw chain when used in the nose-clear down bucking cutting mode. In boring, however, all low-kickback chains exhibited higher operator effort and lower cutting efficiencies than their non-low-kickback counterpart. Considering that most casual chainsaw users primarily work in the down bucking cutting mode, the results suggest that users prioritize safety by selecting low-kickback saw chain. If the user is performing more advanced operations such as boring, then outfitting a non-low-kickback saw chain should be done with cognizance of the safety *vs.* performance tradeoff.

Overall, a generalized testing and analysis procedure for characterizing saw chain cutting performance was developed and then applied in a product comparison study. The usage of a bilinear regression method, tracking of physical properties as a measure of workpiece variability, inclusion of depth-of-cut/physical property interactions, and testing in the boring cutting mode are all new contributions to the field of saw chain cutting mechanics and testing. This work does not attempt to apply analytical cutting mechanics models, such as those introduced by Atkins [44], to the experimental results nor does it take into account effects from grain orientation or chain link geometry in the regression model. Useful expansions to the regression model would be to add in more predictor variables such as cutter link geometry parameters (*e.g.* depth gauge setting and cutter grind angles), wood species, grain orientation, and bumper link geometry parameters. In particular, a predictive model including chain geometry parameters would provide a useful roadmap for engineers when improving or creating new saw chain designs. Furthermore, the presented regression models could be used for matching saw chains with power heads in a process similar to that of Reynolds *et al.* [7,8] but with increased generality with respect to workpiece material properties.

5 BIBLIOGRAPHY

1. Lucia, E., “A Lesson from Nature: Joe Cox and his Revolutionary Saw Chain,” *Forest & Conservation History* 25(3):158–165, 1981, doi:10.2307/4004486.

2. McKenzie, W.M., “The Performance of Gouge Type Power Saw Chains,” *Australian Timber Journal* 21(10):938–954, 1955.

3. Gambrell, S.C.J. and Byars, E.F., “Cutting characteristics of chain saw teeth,” 16(1), 1965.

4. Noguchi, M., Sugihara, H., and Fujii, Y., “Study on the Wood Cutting Ability of a Single Chain-Saw Tooth,” *Journal of the Japanese Forestry Society* 47(8):275–281, 1965.

5. Pahlitzsch, G. and Peters, H., “Investigations on cutting with chain saws-part I: the influence of wood moisture content, cutting direction and feed rate on chain sawing,” *Holz Als Roh-Und Werkstoff* 24(2):59–71, 1966, doi:10.1007/BF02608410.

6. Pahlitzsch, G. and Peters, H., “Investigations on cutting with chain saws part II: the influence of cutting angles and the importance of chip-thickness-limiter on chain sawing,” *Holz Als Roh-Und Werkstoff* 26(10):382–388, 1968, doi:10.1007/BF02615847.

7. Reynolds, D.D., Soedel, W., and Eckelman, C., “Cutting characteristics and power requirements of chain saws.,” *Forest Products Journal* 20(10):28–34, 1970.

8. Reynolds, D.D. and Soedel, W., “Matching of chain saw power requirements with engine characteristics,” *Forest Prod J*, 1972.

9. Stacke, L.-E., “Cutting action of saw chains,” PhD Dissertation, Machine and Vehicle Design, Department of Mechanical Engineering, Chalmers University of Technology, Gothenburg, Sweden, 1989.

10. Naylor, A., Hackney, P., Perera, N., and Clahr, E., “A predictive model for the cutting force in wood machining developed using mechanical properties,” *BioResources* 7(3):2883–2894, 2012, doi:10.15376/biores.7.3.2883-2894.

11. Kivimaa, E., “Cutting Force in Woodworking,” State Institute for Technical Research, Helsinki, 1950.

12. Franz, N., “An Analysis of the Wood-Cutting Process,” University of Michigan Press, Ann Arbor, MI, ISBN 978-0-472-75142-6, 1958.

13. Koch, P., “Wood Machining Processes,” Ronald Press Company, New York, 1964.

14. Cristóvão, L., Broman, O., Grönlund, A., Ekevad, M., and Sitoe, R., “Main cutting force models for two species of tropical wood,” *Wood Material Science and Engineering* 7(3):143–149, 2012, doi:10.1080/17480272.2012.662996.

15. McKenzie, W.M., “Fundamental Analysis of the Wood-Cutting Process,” PhD Dissertation, University of Michigan, Ann Arbor, MI, 1961.

16. Orlowski, K.A., Ochrymiuk, T., Atkins, A., and Chuchala, D., “Application of fracture mechanics for energetic effects predictions while wood sawing,” *Wood Science and Technology* 47(5):949–963, 2013, doi:10.1007/s00226-013-0551-x.

17. Heinzelmann, G., Liebhard, G., and Rosskamp, H., “Energy efficient drive train for a high-performance battery chain saw,” *1st International Electric Drives Production Conference*, IEEE, Nuremburg, ISBN 978-1-4577-1370-5: 101–106, 2011, doi:10.1109/EDPC.2011.6085558.

18. McMillin, C.W. and Lubxin, J.L., “Circular sawing experiments on a radial arm saw,” *Forest Products Journal* 9(10):361–367, 1959.

19. Gronlund, A., “Measuring and Modelling of Cutting Forces,” *9th International Wood Machining Seminar*, University of California Forest Products Laboratory, Richmond, CA: 342–350, 1988.

20. Bucar, B. and Bucar, D.G., “The influence of the specific cutting force and cross-sectional geometry of a chip on the cutting force in the process of circular rip-sawing,” *European Journal of Wood and Wood Products* 60(2):146–151, 2002, doi:10.1007/s00107-002-0281-5.

21. Atkins, T., “Sawing, Chisels and Files,” *The Science and Engineering of Cutting*, Butterworth-Heinemann, Oxford, ISBN 978-0-7506-8531-3: 171–188, 2009, doi:10.1016/B978-0-7506-8531-3.00007-9.

22. Wyeth, D.J., Goli, G., and Atkins, A.G., “Fracture toughness, chip types and the mechanics of cutting wood. A review,” *Holzforschung* 63(2):168–180, 2009, doi:10.1515/HF.2009.017.

23. Oehrli, J.W., “Dynamometer tests on cutting action of chain-saw teeth,” *Forest Products Journal* 10(1):4–7, 1960.

24. Coutermarsh, B.A., “Factors Affecting Rates of Ice Cutting with a Chain Saw,” CRREL-SR-89-24, U.S. Army Cold Regions Research and Engineering Laboratory, Hanover, NH, 1989.

25. Ryan, T.P., “Modern regression methods,” 2nd ed, Wiley, Hoboken, N.J, ISBN 978-0-470-08186-0, 2009.

26. Kretschmann, D.E., “Mechanical Properties of Wood,” *Wood Handbook, Wood as an Engineering Material*, USDA Forest Products Laboratory, Madison, WI, 2010.

27. Chuchala, D., Orlowski, K.A., Sandak, A., Sandak, J., Pauliny, D., and Barański, J., “The Effect of Wood Provenance and Density on Cutting Forces While Sawing Scots Pine (Pinus sylvestris L.),” *BioResources* 9(3), 2014, doi:10.15376/biores.9.3.5349-5361.

28. Haynes, C.D., Webb, W.A., and Fenno, C.R., “Chain Saw Injuries: Review of 330 Cases,” *The Journal of Trauma: Injury, Infection, and Critical Care* 20(9):772–776, 1980, doi:10.1097/00005373-198009000-00011.

29. Koehler, S.A., Luckasevic, T.M., Rozin, L., Shakir, A., Ladham, S., Omalu, B., Dominick, J., and Wecht, C.H., “Death by Chainsaw: Fatal Kickback Injuries to the Neck,” *Journal of Forensic Sciences* 49(2):1–6, 2004, doi:10.1520/JFS2003276.

30. Dąbrowski, A., “Reducing Kickback of Portable Combustion Chain Saws and Related Injury Risks: Laboratory Tests and Deductions,” *International Journal of Occupational Safety and Ergonomics* 18(3):399–417, 2012, doi:10.1080/10803548.2012.11076943.

31. Hammig, B. and Jones, C., “Epidemiology of Chain Saw Related Injuries, United States: 2009 through 2013,” *Advances in Emergency Medicine* 2015:1–4, 2015, doi:10.1155/2015/459697.

32. Brown, A.F., “Chainsaw penetrating neck injury.,” *Emergency Medicine Journal* 12(2):134–137, 1995, doi:10.1136/emj.12.2.134.

33. Koebke, R.H., “Chain Saw Kickback Dynamics,” *Journal of Mechanical Design* 102(2):247, 1980, doi:10.1115/1.3254737.

34. G. T. Roberson and C. W. Suggs, “Construction and Evaluation of a Chainsaw Kickback Simulator,” *Applied Engineering in Agriculture* 7(2):153–157, 1991, doi:10.13031/2013.26224.

35. Arnold, D. and Parmigiani, J.P., “A Study of Chainsaw Kickback,” *Forest Products Journal* 65(5–6):232–238, 2015, doi:10.13073/FPJ-D-14-00096.

36. Donley, R.W., “Cutter chain for power saws,” U.S. Patent 2,826,226, 1958.

37. Carlton, R.R., “Brush cutting chain,” U.S. Patent 3,180,378, 1965.

38. Goldblatt, L., “Kickback-free saw chain,” U.S. Patent 4,133,239, 1979.

39. Arff, U.F., “Saw chain,” U.S. Patent 3,951,027, 1976.

40. Olmr, J.J., “Safety saw chain,” U.S. Patent 4,348,927, 1982.

41. Mang, H., “Saw chain,” U.S. Patent 6,871,573, 2005.

42. Goettel, M. and Way, A., “Saw chain drive link with tail,” U.S. Patent 7,637,192, 2009.

43. Otto, A. and Parmigiani, J.P., “Velocity, Depth-of-Cut, and Physical Property Effects on Saw Chain Cutting,” *BioResources* 10(4):7273–7291, 2015, doi:10.15376/biores.10.4.7273-7291.

44. Atkins, T., “The Science and Engineering of Cutting: The Mechanics and Processes of Separating, Scratching and Puncturing Biomaterials, Metals and Non-metals,” Butterworth-Heinemann, Oxford, ISBN 978-0-08-094245-2, 2009.